IEEE Access
Multidisciplinary | Rapid Review | Open Access Journal

Received July 25, 2021, accepted August 18, 2021, date of publication August 31, 2021, date of current version September 13, 2021.

Digital Object Identifier 10.1109/ACCESS.2021.3109238

Online Non-Collocated Estimation of Payload and Articular Stress for Real-Time Human Ergonomy Assessment

YESHASVI TIRUPACHURI[1], (Member, IEEE), PRASHANTH RAMADOSS[1,2], (Member, IEEE), LORENZO RAPETTI[1,3], (Member, IEEE), CLAUDIA LATELLA[1], (Member, IEEE), KOUROSH DARVISH[1], (Member, IEEE), SILVIO TRAVERSARO[4], (Member, IEEE), AND DANIELE PUCCI[1], (Member, IEEE)

[1]Artificial and Mechanical Intelligence at Istituto Italiano di Tecnologia (IIT), Center for Robotics Technologies, 16163 Genova, Italy
[2]DIBRIS, University of Genoa, 16128 Genova, Italy
[3]Machine Learning and Optimisation, The University of Manchester, Manchester M13 9PL, U.K.
[4]iCub Tech, Center for Robotics Technologies, Istituto Italiano di Tecnologia (IIT), 16163 Genova, Italy

Corresponding author: Yeshasvi Tirupachuri (yeshasvi.tirupachuri@iit.it)

This work was supported by the European Union's Horizon 2020 through the An.Dy project under Agreement 731540 and through the SoftManBot project under Agreement 869855.

ABSTRACT Improving the quality of work for human beings is receiving a lot of attention from multiple research communities. In particular, digital transformation in human factors and ergonomics is going to empower the next generation of the socio-technical workforce. The use of wearable sensors, collaborative robots, and exoskeletons, coupled with novel technologies for the real-time assessment of human ergonomy forms the crux of this digital transformation. In this direction, this paper focuses on the open problem of estimating the interaction wrench experienced at the human extremities (such as hands), where the feasibility of direct sensor measurements is not practical. We refer to our approach as non-collocated wrench estimation, as we aim to estimate the wrench at known contact locations but without using any direct force-torque sensor measurements at these known locations. We achieve this by extending the formulation of stochastic inverse dynamics for humans by considering a centroidal dynamics constraint to perform a reliable non-collocated estimation of interaction wrench and the joint torques (articular stress) experienced as a direct consequence of the interaction. Our approach of non-collocated estimation is thoroughly validated in terms of payload estimation and articular stress estimation through validation and experimental scenarios involving dynamic human motions like walking.

INDEX TERMS Human factors, ergonomics, human–robot interaction, exoskeletons.

I. INTRODUCTION

Despite the recent concerns of automation, the significance of human beings as an integral part of the future socio-technical workforce is being validated through several studies [1], [2]. The rise of digital transformation in human factors and ergonomics enhancement is an indication of targeted focus on improving the quality of work for human beings through wearable sensors, collaborative robots, and exoskeletons, as the complexity of work is increasing [3], [4]. The qualitative assessments that are typically employed in the field of occupational health and safety are limited in their applicability for the new age of Industry 4.0 [5], [6].

Human-Robot Collaboration (HRC) is an example of complex work scenarios, which is considered to be one of the key enabling technologies that truly holds the potential to usher us through Industry 4.0 [7], [8]. The last decade has seen significant research and development efforts in improving robotic systems that are to be deployed alongside human partners, primarily with the focus on the safety and protection of humans. The aspect of human factors and ergonomics enhancement in the context of HRC is slowly gaining attention among interdisciplinary scientific communities [9], [10].

The associate editor coordinating the review of this manuscript and approving it for publication was Tao Liu.

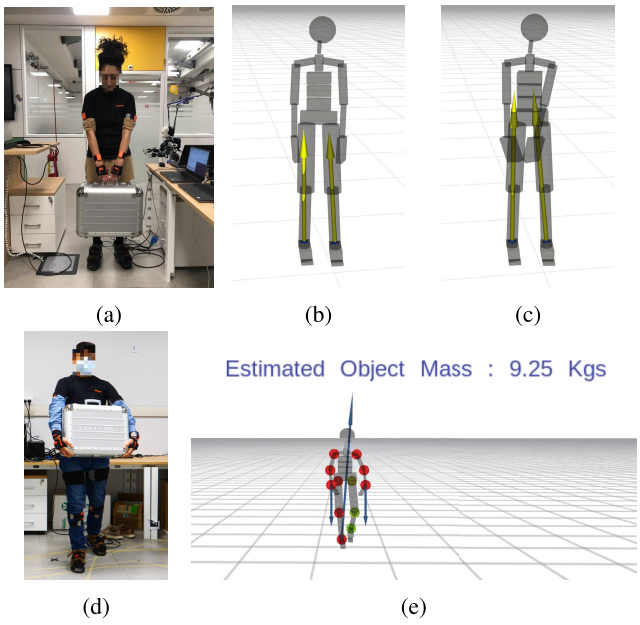

FIGURE 1. **(a) Human subject lifting an external payload of 9.55 kg; (b)-(c) 3D RViz visualization of increase in ground reaction force measurements at the feet of the human model under the influence of payload; (d) An instance of walking motion while carrying the payload; (e) 3D RViz visualization of payload estimation and articular stress estimation. The arrows indicate the external force at the links of the human model, and the scale does not correspond to the magnitude. The spheres at the joints indicate joint efforts.**

Novel tools and techniques that provide continuous, real-time quantitative metrics of a human partner hold the promise to realize truly collaborative scenarios where the robot partners are fully aware of their human partners [11], [12]. Besides that, the lack of standard criteria for the design and performance evaluation of exoskeletons needs to be addressed through quantitative metrics [13]–[15]. Real-time ergonomy assessment is an active research topic that focuses on quantitative metrics to assess and eventually improve the quality of work [16], [17]. Furthermore, standardized and reliable real-time ergonomy assessment is a key enabling technology [18] for realizing many real-world applications with collaborative robots [19], [20], and assistive exoskeletons [14], [21]. Articular stress or joint stress is an important aspect of ergonomy to ensure safe working conditions. Real-time human joint torques estimation is considered in the problem of whole-body human inverse dynamics which has been investigated through different approaches considering different sensor modalities [22]–[25]. Furthermore, incorporating ergonomic optimization during physical collaboration tasks such as manipulating a heavy object is another emerging research direction [26], [27].

Complementary topics of contact detection [28], [29] and contact force estimation [30]–[32] have been an active subject of investigation in robotics literature. Given the system has contact with the environment, the problem of contact detection deals with the localization of the contact, and contact force estimation deals with identifying the strength of the contact. Typically, in the case of human inverse dynamics, rigid contacts at a subject's feet are considered, and the ground reaction force-torque measurements at the feet are important to evaluate the joint torques. However, in some manipulation scenarios such as logistics, the subject carries a payload and an external interaction wrench is experienced at the contact locations of the hands, which in turn affects the internal joint torques under the influence of the payload. The authors of [33] propose an online contact detection and localization method for human ergonomic assessment applications where the weight of the object being manipulated is assumed to be known and only quasi-static movements are considered. An interesting open problem we consider in this work is to estimate the external interaction wrench experienced at human extremities such as hands while manipulating a payload. Particularly, in manipulation scenarios where the user may wear specialized gloves that are safety compliant but do not embed any sensors due to their rugged nature, or in scenarios that require rich tactile perception abilities from direct contact to engage with different tools of the trade. Furthermore, although the recent advances in wearable glove technology are very promising [34], [35], they are still limited in their use for a wide variety of practical applications.

In this work we assume the contact locations to be known, and propose a generalized approach to estimate the external wrench at these known contact locations that are not equipped with any sensors to get direct force-torque measurements. In control theory, scenarios where the actuator and the sensor (providing direct measurements for control) are not positioned (collocated) nearby at the modeling level, are classified as non-collocated problems [36]. We adopt the same terminology and refer to our approach as non-collocated wrench estimation, as we aim to estimate the wrench at known contact locations but without using any direct force-torque sensor measurements at these known locations. Instead, we make use of the force-torque measurements available from the sensors at a different contact location, and this process of non-collocated wrench estimation becomes evident in Section III-A. More importantly, we present the problem formulation as an extension of the stochastic human inverse dynamics method [24] through a two-step approach where the estimation of external wrenches on the links is decoupled from the estimation of internal wrenches exchanged through the joints of the human that results in articular stress. The first step deals with the centroidal dynamics-based non-collocated wrench estimation, followed by the whole-body human dynamics estimation as the second step. A thorough validation of our approach is demonstrated through a set of experimental scenarios where a human subject lifts a payload as shown in Fig. (1a) or (1d), assuming the known contact locations at the hands of the subject.

The main contributions of this manuscript can be summarized as follows,

- Systematic description of stochastic whole-body inverse dynamics problem formulation and its limitation for human articular stress estimation under payloads.

- Extended formulation of stochastic whole-body inverse dynamics through centroidal dynamics constraint in order to achieve non-collocated wrench estimation during external interactions.
- Validation of non-collocated wrench estimation through payload and the associated articular stress estimation.

The rest of the paper is organized as follows: Section II presents the general notation used in the paper followed by the original stochastic inverse dynamics problem formulation and its current limitations. Section III-A describes the general formulation of the stack of tasks stochastic estimation problem, and the extension of the stochastic inverse dynamics problem through centroidal dynamics constraint to achieve non-collocated wrench estimation. Description of the conducted experiments and the discussion of the results that validate the approach are presented in Section IV. In particular, we thoroughly highlight the effect of different parameters that influence the stochastic estimation process. Finally, the concluding remarks that indicate the current limitations and challenges for the real-world application of the proposed approach are discussed in Section V.

II. BACKGROUND

A. NOTATION

- $\boldsymbol{I}_n$ denotes an identity matrix, and $\boldsymbol{0}_n$ denotes a zero matrix of $(n \times n)$ dimensions.
- $\mathcal{I}$ denotes the inertial frame of reference with z-axis pointed against gravity.
- $\boldsymbol{g} = \begin{bmatrix}0 & 0 & -9.81\end{bmatrix}^\top$ denotes the gravity vector expressed in the inertial frame of reference.
- The human is modeled as a rigid multibody *floating base* mechanical system [37] that has N_B rigid bodies as links. Each link pair is connected through three one Degree of Freedom (DoF) rotational joints, that constitute a spherical joint.
- The frame associated to the base link is denoted as $\mathcal{B}$, and the frame associated to the i-th link of the system is denoted as $\mathcal{L}_i$.
- The configuration space of a *free-floating* mechanical system is characterized by the *floating base frame* $\mathcal{B}$ and the *joint positions*. It is defined as a set of elements with 6 dimensions representing the *floating base* and the total number of joints $n = 3 \times (N_B - 1)$. Hence, it lies on the Lie group $\mathbb{Q} = \mathbb{R}^3 \times SO(3) \times \mathbb{R}^n$.
- An element in the configuration space is denoted by $\boldsymbol{q} = (\boldsymbol{q}_\mathcal{B}, \boldsymbol{s}) \in \mathbb{Q}$, which consists of pose of the *base frame* $\boldsymbol{q}_\mathcal{B} = ({}^\mathcal{I}\boldsymbol{p}_\mathcal{B}, {}^\mathcal{I}\boldsymbol{R}_\mathcal{B}) \in \mathbb{R}^3 \times SO(3)$ where ${}^\mathcal{I}\boldsymbol{p}_\mathcal{B} \in \mathbb{R}^3$ denotes the position of the base frame with respect to the inertial frame; ${}^\mathcal{I}\boldsymbol{R}_\mathcal{B} \in SO(3)$ denotes the rotation matrix representing the orientation of the base frame with respect to the inertial frame; and the joint positions vector $\boldsymbol{s} \in \mathbb{R}^n$ which captures the topology, i.e., the internal configuration of the system.
- The system velocity is characterized by the linear and the angular velocity of the *base frame* along with the *joint velocities*. Accordingly, the configuration velocity space lies on the group $\mathbb{V} = \mathbb{R}^3 \times \mathbb{R}^3 \times \mathbb{R}^n$. An element of the configuration velocity space $\nu \in \mathbb{V}$ is defined as $\nu = (\boldsymbol{v}_\mathcal{B}, \dot{\boldsymbol{s}})$, where $\boldsymbol{v}_\mathcal{B} = ({}^\mathcal{I}\dot{\boldsymbol{p}}_\mathcal{B}, {}^\mathcal{I}\boldsymbol{\omega}_\mathcal{B}) \in \mathbb{R}^3 \times \mathbb{R}^3$ denotes the linear and angular velocity of the *base frame*, and $\dot{\boldsymbol{s}} \in \mathbb{R}^n$ denotes the joint velocities.
- The operator $S(.) : \mathbb{R}^3 \to \mathfrak{so}(3)$ maps 3D vectors to *skew − symmetric* matrices, such that given two vectors $\boldsymbol{v}, \boldsymbol{u} \in \mathbb{R}^3$, it is defined as $\boldsymbol{v} \times \boldsymbol{u} = S(\boldsymbol{v})\boldsymbol{u}$, where $\times$ is the cross-product operator.
- The *vee* operator $.^\vee : \mathfrak{so}(3) \to \mathbb{R}^3$ denotes the inverse of the *skew-symmetric* operator, such that given a matrix $\boldsymbol{A} \in \mathfrak{so}(3)$ and a vector $\boldsymbol{u} \in \mathbb{R}^3$, it is defined as $\boldsymbol{A}\boldsymbol{u} = \boldsymbol{A}^\vee \times \boldsymbol{u}$.
- The estimate of a quantity is indicated with $\widehat{\ }$ placed on top of the symbol, such as $\widehat{(\cdot)}$.

B. STOCHASTIC INVERSE DYNAMICS

A stochastic formulation of the inverse dynamics estimation problem for a whole-body fixed-base human model was first investigated in [25], [38] and later extended to a floating base human model in our recent work [24]. The central idea of the stochastic human dynamics estimation approach is to define a dynamic variables vector $\boldsymbol{d}$ that is composed of accelerations and kinetic quantities, i.e., the external forces and torques (wrenches) acting on the human subject.

1) DYNAMIC VARIABLES

The dynamic variables vector $\boldsymbol{d}$ is defined as,

$$\boldsymbol{d} = \begin{bmatrix}\boldsymbol{d}_{link}^\top & \boldsymbol{d}_{joint}^\top\end{bmatrix}^\top \in \mathbb{R}^{12N_B+7n}, \tag{1}$$

where, $\boldsymbol{d}_{link} \in \mathbb{R}^{12N_B}$ and $\boldsymbol{d}_{joint} \in \mathbb{R}^{7n}$, are defined as,

$$\boldsymbol{d}_{link} = \begin{bmatrix}\boldsymbol{\alpha}_0^g & \boldsymbol{f}_0^x & \dots & \boldsymbol{\alpha}_{N_B-1}^g & \boldsymbol{f}_{N_B-1}^x\end{bmatrix}, \tag{2a}$$

$$\boldsymbol{d}_{joint} = \begin{bmatrix}\boldsymbol{f}_{J_1} & \dots & \boldsymbol{f}_{J_n} & \ddot{s}_1 & \dots & \ddot{s}_n\end{bmatrix}, \tag{2b}$$

where, $\boldsymbol{\alpha}_i^g \in \mathbb{R}^6$ denotes the proper acceleration [24] of the i-th link, and $\boldsymbol{f}_i^x$ denotes the external wrench acting on the i-th link, which is emphasized by the superscript x. The link quantities are expressed in their body frame. $\boldsymbol{f}_{J_i}$ denotes the internal wrench exchanged through the i-th joint, and $\ddot{s}_i$ denotes the acceleration of the i-th joint. These dynamic variables are estimated by exploiting the kinematic and the dynamic model constraints of the system along with the sensor measurements.

2) SENSOR MEASUREMENTS

Human biomechanical analysis requires kinematic information such as position, velocity, and acceleration of various body parts that can be obtained through different sensory modalities such as marker-based optical tracking or inertial tracking systems. Furthermore, the ground reaction forces and torques at the feet of the human are the kinetic information that is typically measured through force-torque platforms. Given the definition of the dynamic variables vector $\boldsymbol{d}$, we consider proper acceleration measurements ${}^m\boldsymbol{a}^g \in \mathbb{R}^3$,

and wrench measurements ${}^m\boldsymbol{f}^x \in \mathbb{R}^6$ as sensor measurement inputs. Note the superscript ${}^m(.)$ denotes a measured quantity. Let us consider N_s^a number of inertial measurement units (IMUs) that provide acceleration measurements and assume the net external wrench acting on all the links of the model i.e., N_B are available as measurement inputs. The total number of "sensors" considered is denoted as $N_s = N_s^a + N_B$. The measurement vector $\boldsymbol{y} \in \mathbb{R}^{3\,N_s^a+6\,N_B}$ is denoted as,

$$\boldsymbol{y} = \begin{bmatrix} ({}^m\boldsymbol{a}_0^g)^\top & \cdots & ({}^m\boldsymbol{a}_{N_s^a}^g)^\top & ({}^m\boldsymbol{f}_0^x)^\top & \cdots & ({}^m\boldsymbol{f}_{N_{B-1}}^x)^\top \end{bmatrix}^\top \quad (3)$$

3) OPTIMIZATION PROBLEM

The dynamic variables $\boldsymbol{d}$ and the measurements $\boldsymbol{y}$ are considered to be stochastic variables with Gaussian distributions. The estimation of dynamic variables $\boldsymbol{d}$ problem is posed as finding the Maximum A-Posteriori (MAP) estimate by maximizing the conditional probability distribution of the dynamic variables $\boldsymbol{d}$ given the measurements $\boldsymbol{y}$, and the prior knowledge of the system encapsulated through the model constraints. Now, the stochastic inverse dynamics problem when posed as an optimization problem is represented by (4), as shown at the bottom of the page, where $\boldsymbol{D} \in \mathbb{R}^{(18\,N_B+n)\times(12\,N_B+7\,n)}$ is a model-constrained block matrix, $\boldsymbol{b}_D \in \mathbb{R}^{18\,N_B+n}$ is a model bias vector, $\boldsymbol{Y} \in \mathbb{R}^{N_s\times(12N_B+7n)}$ is a measurement block matrix and $\boldsymbol{b}_Y \in \mathbb{R}^{N_s}$ is a measurement bias vector. The detailed examination of the model constraints equation and the measurements equation is beyond the scope of this manuscript. The reader is advised to refer to Chapter 4 of [25] for further details.

4) COVARIANCE EFFECT

Given the structure of the optimization problem presented in (4), the solution of the dynamic variables estimation is influenced by three covariances: *i*) prior covariance $\boldsymbol{\Sigma}_d$, *ii*) measurement covariance $\boldsymbol{\Sigma}_y$, and *iii*) model covariance $\boldsymbol{\Sigma}_D$. The effect of these covariances on the estimation can be summarized as:

- Prior covariance $\boldsymbol{\Sigma}_d$ influences the change of the dynamic variables with respect to the prior mean $\boldsymbol{\mu}_d$.
- Model covariance $\boldsymbol{\Sigma}_D$ influences the consistency of the dynamic variable estimates with respect to the model constraints.
- Measurement covariance $\boldsymbol{\Sigma}_y$ influences some of the dynamic variable's convergence towards their associated sensor measurements in $\boldsymbol{y}$.

The combined contribution of this set of covariances results in the estimation of dynamic variables denoted as,

$$\boldsymbol{d}^{\text{MAP}} = \begin{bmatrix} \widehat{\boldsymbol{d}}_{link}^\top & \widehat{\boldsymbol{d}}_{joint}^\top \end{bmatrix}^\top, \quad (5)$$

$$\widehat{\boldsymbol{d}}_{link} = \begin{bmatrix} \widehat{\boldsymbol{\alpha}}_0^g & \widehat{\boldsymbol{f}}_0^x & \cdots & \widehat{\boldsymbol{\alpha}}_{N_{B-1}}^g & \widehat{\boldsymbol{f}}_{N_{B-1}}^x \end{bmatrix}, \quad (6a)$$

$$\widehat{\boldsymbol{d}}_{joint} = \begin{bmatrix} \widehat{\boldsymbol{f}}_{J_1} & \cdots & \widehat{\boldsymbol{f}}_{J_n} & \widehat{\dot{s}}_1 & \cdots & \widehat{\dot{s}}_n \end{bmatrix}. \quad (6b)$$

C. CURRENT LIMITATION

This section details the limitations of the original stochastic inverse dynamics approach presented in Section II-B in relation to the interaction wrench experienced by the payload carried by a human subject, and the associated joint torques. To explain the concepts further, let us consider a set of frames $\boldsymbol{\mathcal{L}} = \{\mathcal{L}_0, \mathcal{L}_1, \mathcal{L}_2, \ldots, \mathcal{L}_{N_{B-1}}\}$ that are associated with all the links of the human model. Let $\boldsymbol{\mathcal{F}} \subset \boldsymbol{\mathcal{L}}$ be the subset that contains the links associated with the feet, and $\boldsymbol{\mathcal{H}} \subset \boldsymbol{\mathcal{L}}$ be the subset that contains the links associated with the hands. The subset $\boldsymbol{\mathcal{U}} \subset \boldsymbol{\mathcal{L}}$ contains all the frames excluding the frames associated with the feet and hand links. Given these definitions, the set of all the frames is the union of the three disjoint subsets, i.e., $\boldsymbol{\mathcal{L}} = \left(\boldsymbol{\mathcal{F}} \cup \boldsymbol{\mathcal{H}} \cup \boldsymbol{\mathcal{U}}\right)$.

The current formulation of the stochastic inverse dynamics estimation problem presented in Section II-B assumes that only the feet links of the human are in contact with the environment and the external wrench at the feet ${}^m\boldsymbol{f}_{\mathcal{L}\in\boldsymbol{\mathcal{F}}}^x$ are obtained through the force-torque sensor measurements. Assuming that no external wrench is present on any other links, the external wrench measurements ${}^m\boldsymbol{f}_{\mathcal{L}\in(\boldsymbol{\mathcal{H}}\cup\boldsymbol{\mathcal{U}})}^x$ for the rest of the links is set to zero, i.e., $\boldsymbol{0}_{6\times1}$. The measurement covariance for link external wrenches $\boldsymbol{\Sigma}_y^{f^x}$ are chosen to a very low value such that the estimates of the external wrench at the feet links $\widehat{\boldsymbol{f}}_{\mathcal{L}\in\boldsymbol{\mathcal{F}}}^x$ are as close as possible to the input measurements ${}^m\boldsymbol{f}_{\mathcal{L}\in\boldsymbol{\mathcal{F}}}^x$ represented by (7a). This point becomes evident from the discussion of results presented in Section IV-C1.

Similarly, the estimates of the external wrench at all the other links $\widehat{\boldsymbol{f}}_{\mathcal{L}\in(\boldsymbol{\mathcal{H}}\cup\boldsymbol{\mathcal{U}})}^x$ are close to their assumed zero-measurements, represented by (7b)-(7c).

$$\widehat{\boldsymbol{f}}_{\mathcal{L}\in\boldsymbol{\mathcal{F}}}^x \approx {}^m\boldsymbol{f}_{\mathcal{L}\in\boldsymbol{\mathcal{F}}}^x, \quad (7a)$$

$$\widehat{\boldsymbol{f}}_{\mathcal{L}\in\boldsymbol{\mathcal{H}}}^x \approx {}^m\boldsymbol{f}_{\mathcal{L}\in\boldsymbol{\mathcal{H}}}^x = \boldsymbol{0}_{6\times1}, \quad (7b)$$

$$\widehat{\boldsymbol{f}}_{\mathcal{L}\in\boldsymbol{\mathcal{U}}}^x \approx {}^m\boldsymbol{f}_{\mathcal{L}\in\boldsymbol{\mathcal{U}}}^x = \boldsymbol{0}_{6\times1}. \quad (7c)$$

Now, let us consider an example scenario where the human is lifting a payload such as a heavy object as shown in Fig. (1a). When the object is handled, the additional weight of the object is reflected in the ground reaction forces

$$\boldsymbol{d}^{\text{MAP}} = \arg\min_{\boldsymbol{d}} \left(\underbrace{||\boldsymbol{D}\boldsymbol{d} + \boldsymbol{b}_D||^2_{\boldsymbol{\Sigma}_D^{-1}}}_{\text{Model}} + \underbrace{||\boldsymbol{Y}\boldsymbol{d} + \boldsymbol{b}_Y - \boldsymbol{y}||^2_{\boldsymbol{\Sigma}_y^{-1}}}_{\text{Measurements}} + \underbrace{||\boldsymbol{d} - \boldsymbol{\mu}_d||^2_{\boldsymbol{\Sigma}_d^{-1}}}_{\text{Prior}} \right). \quad (4)$$

at the feet as shown by the increase of the yellow arrows in Fig. (1b)-(1c). Under such circumstances, the subject experiences external interaction wrench at the hands that correspond to the payload weight, and it further affects the associated internal joint torques. In such a scenario, rather than forcing the wrench estimates at the hand links $\widehat{\boldsymbol{f}}^x_{\mathcal{L}\in\mathcal{H}}$ toward their assumed zero measurements, we consider the problem of estimating the external interaction wrench that reflects the weight of the payload, and estimate the internal articular stress under the influence of the payload. This problem is referred to as the non-collocated wrench estimation as it deals with the wrench estimation on links that do not have any direct force-torque sensor measurements.

Considering the current formulation of the estimation problem represented by (4), the wrench estimates at the hand links $\widehat{\boldsymbol{f}}^x_{\mathcal{L}\in\mathcal{H}}$ can be influenced only through their measurement covariance value. However, the measurement covariance can be tuned to either push the estimates to be close to their set measurement of $\mathbf{0}_{6\times1}$ or away from it. Moreover, the estimated wrench at the hands will not reflect the payload that is held by the human subject, and this will become evident during the discussion of the results presented in Section. IV-C2. Furthermore, given the definition of the dynamic variables vector $\boldsymbol{d}$ from (1), the estimation of external link wrench variables $\boldsymbol{f}^x$ and the internal joint wrench variables $\boldsymbol{f}_j$ is coupled through the model constraints. This coupling renders it difficult to adjust the model and measurement covariances to achieve non-collocated wrench estimation for estimating the external interaction wrench at the hands experienced by the human subject while handling a payload, and the associated joint torques under the influence of the payload.

In addition to the limitations mentioned above, the current formulation assumes that the state information of the system, i.e. $\boldsymbol{x} = \left[\boldsymbol{s}^\top \dot{\boldsymbol{s}}^\top\right]^\top$ is available as a measurement without uncertainty. As some of the measurements and model constraints are state-dependent, any noise in the state information eventually affects the estimation of the dynamic variables. Hence, the state estimation needs to be formulated as a part of the stochastic framework to account for the noise in the state information. An initial investigation of simultaneous state and dynamics stochastic estimation is carried in [39] with limited offline validation results using a fixed-base articulated humanoid robot as an experimental platform. Online implementation of state and dynamics stochastic estimation for highly articulate floating-base systems like humans is yet to be realized and validated.

The limitations highlighted so far can be addressed by reformulating the original stochastic estimation problem as a hierarchical stack of tasks formulation. Furthermore, the main contribution of extended formulation of stochastic whole-body inverse dynamics problem through centroidal dynamics constraint is presented in detail in the next section.

III. STACK OF TASKS STOCHASTIC ESTIMATION

Looking at the original stochastic estimation problem represented by (4), it is evident that the estimation is focused on the entire set of dynamic variables vector $\boldsymbol{d}$. Such a consideration proved to be difficult to tune the various covariance values to achieve a physically consistent estimation of different dynamic variables. Hence, a general framework composed of a stack of tasks stochastic estimation formulation allows for an intuitive covariance tuning. Towards realizing such a general formulation, let us first consider the internal state variables vector denoted as,

$$\boldsymbol{x} = \left[\boldsymbol{s}^\top \quad \dot{\boldsymbol{s}}^\top\right]^\top. \tag{8}$$

The internal state variables of the vector $\boldsymbol{x}$ are considered to be stochastic variables with Gaussian distributions. Now, let us consider a forward kinematics model denoted as $FK(\boldsymbol{x})$ [40], [41], and the target kinematic measurements of link pose $\boldsymbol{q}_{\mathcal{L}}$ and link velocity $\boldsymbol{v}_{\mathcal{L}}$ denoted as,

$$\boldsymbol{y}_{kinematic} = \left[\boldsymbol{q}^\top_{\mathcal{L}_i} \quad \boldsymbol{v}^\top_{\mathcal{L}_i}\right]^\top \quad \forall i \in [1, \ldots, N_B]. \tag{9}$$

Note that the internal state estimates allow us to compute the quantities necessary for the higher-level tasks. Now, let us consider the measurement vector $\boldsymbol{y}_k$ that is composed of all the external link wrenches acting on the systems, i.e.,

$$\boldsymbol{y}_k = \left[({}^m\boldsymbol{f}^x_0)^\top \quad \ldots \quad ({}^m\boldsymbol{f}^x_{N_B-1})^\top\right]^\top. \tag{10}$$

Similarly, a dynamic variables vector composed of only the external link wrenches is denoted as,

$$\boldsymbol{d}_k = \left[(\boldsymbol{f}^x_0)^\top \quad (\boldsymbol{f}^x_1)^\top \quad \ldots \quad (\boldsymbol{f}^x_{N_B-1})^\top\right]^\top. \tag{11}$$

Given the previous definitions from (1)-(3), and (8)-(11), a general stack of tasks stochastic estimation problem is represented by (12a)–(12c), as shown at the bottom of the next page. Such a hierarchical formulation ensures the state estimation followed by the kinetics, and the estimation of the full dynamic variables vector with the possibility to account for uncertainty at each level. The research topic of online stochastic state estimation for highly articulated systems like humans is under active research in the biomechanics community [42], and it is not the central topic of this manuscript. So, the next section highlights the exact details of exploiting the stack of tasks formulation to address the particular problem of non-collocated wrench estimation.

A. NON-COLLOCATED WRENCH ESTIMATION

Given the general stack of tasks stochastic estimation problem represented by (12), it is to be noted that the external link wrench variables are decoupled from the internal joint wrench variables by considering the kinetics estimation problem. Furthermore, the limitations of guiding the hand's wrench estimation towards the payload are realized by considering centroidal dynamics as a new constraint.

The Centroidal dynamics of a rigid multibody system is influenced only by the external wrench on the links of the system while it is not affected by the internal joint wrenches [43]. This effectively decouples the estimation of the external link wrench and the internal joint wrench variables. More importantly, centroidal dynamics constraint relates the external

$$\boldsymbol{d}^{\text{MAP}} = \underbrace{\arg\min_{\boldsymbol{d}}(||\boldsymbol{D}\boldsymbol{d}+\boldsymbol{b}_D||^2_{\boldsymbol{\Sigma}_D^{-1}} + ||\boldsymbol{Y}\boldsymbol{d}+\boldsymbol{b}_Y-\boldsymbol{y}||^2_{\boldsymbol{\Sigma}_y^{-1}} + ||\boldsymbol{d}-\boldsymbol{\mu}_d||^2_{\boldsymbol{\Sigma}_d^{-1}})}_{\text{Dynamics Estimation Problem}}, \quad s.t. \tag{12a}$$

$$\boldsymbol{d}_k^{\text{MAP}} = \underbrace{\arg\min_{\boldsymbol{d}_k}(||\boldsymbol{Y}_k\boldsymbol{d}_k+\boldsymbol{b}_{Y_k}-\boldsymbol{y}_k||^2_{\boldsymbol{\Sigma}_{y_k}^{-1}} + ||\boldsymbol{d}_k-\boldsymbol{\mu}_{d_k}||^2_{\boldsymbol{\Sigma}_{d_k}^{-1}})}_{\text{Kinetics Estimation Problem}}, \quad s.t. \tag{12b}$$

$$\boldsymbol{x}^{\text{MAP}} = \underbrace{\arg\min_{\boldsymbol{x}}(||FK(\boldsymbol{x}) - \boldsymbol{y}_{kinematic}||^2_{\boldsymbol{\Sigma}^{-1}_{y_{kinematic}}} + ||\boldsymbol{x}-\boldsymbol{\mu}_x||^2_{\boldsymbol{\Sigma}_x^{-1}})}_{\text{State Estimation Problem}}. \tag{12c}$$

wrench acting on the links of the system, which enables us to perform non-collocated wrench estimation for links such as hands, using the increase in feet wrench measurements under the influence of a payload. The *centroidal* frame is a unique coordinate frame with its origin at the center of mass of the system and its orientation is the same as the orientation of the inertial frame of reference [44]. The centroidal frame is denoted by $\mathcal{G}[\mathcal{I}]$ or $\bar{\mathcal{G}}$. Centroidal dynamics relate the rate of change of momentum of the system to the sum of all the external wrenches acting on the system defined by the following relation,

$$\dot{}^{\bar{\mathcal{G}}}\boldsymbol{h} = \sum_{i=1}^{N_B} {}^{\bar{\mathcal{G}}}\boldsymbol{f}^x_{\mathcal{L}_i} + \begin{bmatrix} m\,\boldsymbol{g} \\ 0_{3\times 1} \end{bmatrix}, \tag{13}$$

where, $\dot{}^{\bar{\mathcal{G}}}\boldsymbol{h} \in \mathbb{R}^{6\times 1}$ denotes the rate of change of centroidal momentum, ${}^{\bar{\mathcal{G}}}\boldsymbol{f}^x_{\mathcal{L}_i}$ denotes the external wrench acting on the i-th link expressed in the centroidal frame, and m denotes the mass of the human subject. Now, let us denote the gravity wrench vector as ${}^{\bar{\mathcal{G}}}\boldsymbol{w} = \begin{bmatrix} m\,\boldsymbol{g}^\top & 0_{1\times 3} \end{bmatrix}^\top$, and (13) can be rearranged as,

$$\dot{}^{\bar{\mathcal{G}}}\underline{\boldsymbol{h}} = \sum_{i=1}^{N_B} {}^{\bar{\mathcal{G}}}\boldsymbol{f}^x_{\mathcal{L}_i}, \tag{14}$$

where, $\dot{}^{\bar{\mathcal{G}}}\underline{\boldsymbol{h}} = \dot{}^{\bar{\mathcal{G}}}\boldsymbol{h} - {}^{\bar{\mathcal{G}}}\boldsymbol{w} \in \mathbb{R}^{6\times 1}$.

The centroidal momentum of the system, i.e., the momentum about the center of mass, can be computed as the sum of the individual link momentum through kinematic approach [45] given by,

$${}^{\bar{\mathcal{G}}}\boldsymbol{h} = \sum_{\mathcal{L}\in\mathcal{L}} {}^{\bar{\mathcal{G}}}\boldsymbol{X}^*_{\mathcal{L}}\, {}_{\mathcal{L}}\boldsymbol{I}_{\mathcal{L}}\, {}^{\mathcal{L}}\boldsymbol{v}_{\mathcal{L}}, \tag{15}$$

where ${}^{\bar{\mathcal{G}}}\boldsymbol{X}^*_{\mathcal{L}} \in \mathbb{R}^{6\times 6}$ is an adjoint wrench transformation matrix, ${}^{\mathcal{L}}\boldsymbol{v}_{\mathcal{L}}$ is the velocity of the i-th link, and ${}_{\mathcal{L}}\boldsymbol{I}_{\mathcal{L}}$ is the 6D inertia of the i-th link expressed in the body frame and denoted as,

$${}_{\mathcal{L}}\boldsymbol{I}_{\mathcal{L}} = \begin{bmatrix} m_{\mathcal{L}}\boldsymbol{I}_3 & -m_{\mathcal{L}}\mathbf{S}({}^{\mathcal{L}}\boldsymbol{c}_{\mathcal{L}}) \\ m_{\mathcal{L}}\mathbf{S}({}^{\mathcal{L}}\boldsymbol{c}_{\mathcal{L}}) & \bar{\boldsymbol{I}}_{\mathcal{L}} \end{bmatrix}.$$

$m_{\mathcal{L}} \in \mathbb{R}$ is the mass of the link, ${}^{\mathcal{L}}\boldsymbol{c}_{\mathcal{L}} \in \mathbb{R}^3$ denotes the center of mass with respect to the body frame of the link, and $\bar{\boldsymbol{I}}_{\mathcal{L}} \in \mathbb{R}^{3\times 3}$ denotes the 3D inertia of the link expressed with respect to the body frame. On taking the time derivative of the centroidal momentum (15), the rate of change of centroidal momentum is expressed as,

$$\dot{}^{\bar{\mathcal{G}}}\boldsymbol{h} = \sum_{\mathcal{L}\in\mathcal{L}} \dot{}^{\bar{\mathcal{G}}}\boldsymbol{X}^*_{\mathcal{L}}\, {}_{\mathcal{L}}\boldsymbol{I}_{\mathcal{L}}\, {}^{\mathcal{L}}\boldsymbol{v}_{\mathcal{L}} + \sum_{\mathcal{L}\in\mathcal{L}} {}^{\bar{\mathcal{G}}}\boldsymbol{X}^*_{\mathcal{L}}\, {}_{\mathcal{L}}\boldsymbol{I}_{\mathcal{L}}\, {}^{\mathcal{L}}\dot{\boldsymbol{v}}_{\mathcal{L}}, \tag{16}$$

where ${}^{\mathcal{L}}\dot{\boldsymbol{v}}_{\mathcal{L}} \in \mathbb{R}^6$ denotes the acceleration of the i-th link, and $\dot{}^{\bar{\mathcal{G}}}\boldsymbol{X}^*_{\mathcal{L}} = {}^{\bar{\mathcal{G}}}\boldsymbol{X}^*_{\mathcal{L}}\, {}^{\mathcal{L}}\boldsymbol{v}_{\mathcal{L}}\bar{\times}^*$

$${}^{\mathcal{L}}\boldsymbol{v}_{\mathcal{L}}\bar{\times}^* := \begin{bmatrix} \mathbf{S}({}^{\mathcal{L}}\boldsymbol{\omega}_{\mathcal{L}}) & \mathbf{0}_3 \\ \mathbf{S}({}^{\mathcal{L}}\mathbf{v}_{\mathcal{L}}) & \mathbf{S}({}^{\mathcal{L}}\boldsymbol{\omega}_{\mathcal{L}}) \end{bmatrix}.$$

The consideration of centroidal dynamics as a new constraint enables us to develop a version of the stack of tasks stochastic estimation problems to achieve non-collocated wrench estimation. Let us consider a new measurement vector $\boldsymbol{y}' \in \mathbb{R}^{6N_B+6}$ with the measurements of external wrench on the links, expressed in the body frame and an additional "sensor" input of $\dot{}^{\bar{\mathcal{G}}}\underline{\boldsymbol{h}}$ is considered as,

$$\boldsymbol{y}' = \begin{bmatrix} \boldsymbol{y}_k & \dot{}^{\bar{\mathcal{G}}}\underline{\boldsymbol{h}}^\top \end{bmatrix}^\top. \tag{17}$$

Based on the choice of $\boldsymbol{d}'$ and $\boldsymbol{y}'$, the structure of the block diagonal matrix $\boldsymbol{Y}' \in \mathbb{R}^{(6\times(N_B+1))\times(6\times N_B)}$ becomes,

$$\boldsymbol{Y}' = \begin{bmatrix} \boldsymbol{I}_6 & \mathbf{0}_6 & \dots & \mathbf{0}_6 \\ \vdots & \vdots & \vdots & \vdots \\ \mathbf{0}_6 & \mathbf{0}_6 & \dots & \boldsymbol{I}_6 \\ {}^{\bar{\mathcal{G}}}\boldsymbol{X}^*_{\mathcal{L}_0} & {}^{\bar{\mathcal{G}}}\boldsymbol{X}^*_{\mathcal{L}_1} & \dots & {}^{\bar{\mathcal{G}}}\boldsymbol{X}^*_{\mathcal{L}_{N_B-1}} \end{bmatrix}, \tag{18}$$

where, ${}^{\bar{\mathcal{G}}}\boldsymbol{X}^*_{\mathcal{L}_i} \in \mathbb{R}^{6\times 6}$ is an adjoint wrench matrix transformation from the i-th link body frame to the centroidal frame. Now, a new optimization problem considering only the kinetics and the centroidal dynamics equation is defined as,

$$\boldsymbol{d}_k^{\text{MAP}} = \arg\min_{\boldsymbol{d}_k} \Big(\underbrace{||\boldsymbol{Y}'\boldsymbol{d}_k - \boldsymbol{y}'||^2_{\boldsymbol{\Sigma}^{-1}_{y'}}}_{\text{Measurements}} + \underbrace{||\boldsymbol{d}_k - \boldsymbol{\mu}_{d_k}||^2_{\boldsymbol{\Sigma}^{-1}_{d_k}}}_{\text{Prior}} \Big). \tag{19}$$

The optimization problem presented in (19) does not consider the model constraints, and as a result, the external link wrench estimation and the internal joint wrench estimation are decoupled. More importantly, it relates the wrench at links where we have direct sensor measurements, such as feet, and the wrench at links where we do not have direct sensor measurements, such as hands. This effectively facilitates non-collocated wrench estimation. Following the measurement covariance tuning explained in section II-B4, the link external wrench estimates at the feet and all the other links, except for the hand links are forced towards the measurements (from assumed values or sensor readings),

$$\widehat{\boldsymbol{f}}^{x}_{\mathcal{L}\in\mathcal{F}} \approx {}^{m}\boldsymbol{f}^{x}_{\mathcal{L}\in\mathcal{F}}, \tag{20a}$$

$$\widehat{\boldsymbol{f}}^{x}_{\mathcal{L}\in\mathcal{U}} \approx {}^{m}\boldsymbol{f}^{x}_{\mathcal{L}\in\mathcal{U}} = \mathbf{0}_{6\times 1}. \tag{20b}$$

Concerning the wrench estimates at the hand links, the effect of centroidal dynamics constraints added as a part of the optimization problem of (19) can be explained analytically as following,

$$\sum_{\mathcal{L}\in\boldsymbol{\mathcal{U}}} {}^{\bar{\mathcal{G}}}\boldsymbol{X}^{*}_{\mathcal{L}}\widehat{\boldsymbol{f}}^{x}_{\mathcal{L}} + \sum_{\mathcal{L}\in\boldsymbol{\mathcal{F}}} {}^{\bar{\mathcal{G}}}\boldsymbol{X}^{*}_{\mathcal{L}}\widehat{\boldsymbol{f}}^{x}_{\mathcal{L}} + \sum_{\mathcal{L}\in\boldsymbol{\mathcal{H}}} {}^{\bar{\mathcal{G}}}\boldsymbol{X}^{*}_{\mathcal{L}}\widehat{\boldsymbol{f}}^{x}_{\mathcal{L}} = {}^{\bar{\mathcal{G}}}\underline{\dot{\boldsymbol{h}}}. \tag{21}$$

Using the estimates from (20a) and (20b) in the relation (21), we get,

$$\sum_{\mathcal{L}\in\boldsymbol{\mathcal{H}}} {}^{\bar{\mathcal{G}}}\boldsymbol{X}^{*}_{\mathcal{L}}\widehat{\boldsymbol{f}}^{x}_{\mathcal{L}} = {}^{\bar{\mathcal{G}}}\underline{\dot{\boldsymbol{h}}} - \sum_{\mathcal{L}\in\boldsymbol{\mathcal{F}}} {}^{\bar{\mathcal{G}}}\boldsymbol{X}^{*}_{\mathcal{L}}\,{}^{m}\boldsymbol{f}^{x}_{\mathcal{L}}. \tag{22}$$

The relation (22) guides the external wrench estimates at the hand links to reflect the wrench experienced under the weight of the payload such as in an example scenario as shown in Fig. 1. To understand the process of non-collocated wrench estimation more intuitively, let us consider the payload handling scenario as indicated in Fig. 2. The top row indicates the subject standing without any payload, and with a payload held at the hands. The bottom row indicates the 3D visualization of the human model corresponding to the instances shown in the top row. The arrows on the feet indicate the measured external interaction wrench (yellow-colored), and the estimated external interaction wrench (blue-colored) at the feet links of the human that are in contact with the environment. Now, following the relation (7a) the estimated interaction wrench and the measured interaction wrench at the feet are nearly matching. This fact is highlighted and discussed quantitatively in Section IV-C1. The interaction wrench experienced at the feet under the influence of a payload corresponds to the weight of the subject and the weight of the payload combined. This fact is highlighted by a green double-sided arrow to show the slight increase in the length of the wrench arrows at the feet. Now, following the relation (22) this increase in the interaction wrench at the feet that corresponds to the weight of the payload is reflected as the estimated interaction wrench at the hands. This process of estimating the interaction wrench at the contact locations that do not have any direct sensor measurements, using force-torque measurements from sensors at another contact location is referred to as non-collocated wrench estimation. Detailed visualization of non-collocated wrench estimation process is highlighted in Fig. 15 from Section IV.

The resulting estimates of the dynamic variables from (19) are denoted as,

$$\boldsymbol{d}^{\text{MAP}}_{k} = \begin{bmatrix} \widehat{\boldsymbol{f}}^{x}_{0} & \widehat{\boldsymbol{f}}^{x}_{1} & \dots & \widehat{\boldsymbol{f}}^{x}_{N_{B}-1} \end{bmatrix}. \tag{23}$$

The original estimation problem represented by (4) can be decomposed into a two-step process as presented in (25). The non-collocated wrench estimation represented by (25a) and (25b), as shown at the bottom of the next page, is considered to be the first step that results in link external wrench estimates (23). These estimates are given as the input wrench

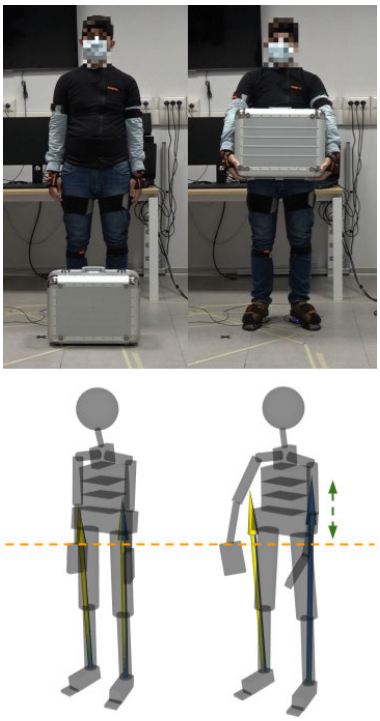

FIGURE 2. Payload handling example scenario to highlight the process of non-collocated wrench estimation. The top row indicates the subject standing without any payload, and with a payload held at the hands. The bottom row indicates the 3D visualization of the human model corresponding to the instances shown in the top row. The arrows are the feet indicate the external interaction wrench at the feet links of the human that are in contact with the environment. Yellow-colored arrows indicate the interaction wrench measured through direct sensor measurements, while the blue-colored arrows indicate the estimated interaction wrench. Note that the arrow representation of the interaction wrench is a qualitative representation rather than a quantitative representation. So, the length of the arrow does not represent the exact magnitude of the interaction wrench. The interaction wrench experienced at the feet under the influence of a payload corresponds to the weight of the subject and the weight of the payload combined. This fact is highlighted by a green double-sided arrow to show the slight increase in the length of the wrench arrows at the feet.

Updated Dynamics Estimation Problem

$$\boldsymbol{d}^{\text{MAP}} = \arg\min_{d}(||\boldsymbol{D}\boldsymbol{d}+\boldsymbol{b}_D||^2_{\boldsymbol{\Sigma}_D^{-1}} + ||\boldsymbol{Y}\boldsymbol{d}+\boldsymbol{b}_Y - \boldsymbol{y}^{''}||^2_{\boldsymbol{\Sigma}_y^{-1}} + ||\boldsymbol{d}-\boldsymbol{\mu}_d||^2_{\boldsymbol{\Sigma}_d^{-1}}), \quad \text{(25a)}$$

$$s.t.$$

Non-Collocated Wrench Estimation

$$\boldsymbol{d}_k^{\text{MAP}} = \arg\min_{d_k}(||\boldsymbol{Y}^{'}\boldsymbol{d}_k - \boldsymbol{y}^{'}||^2_{\boldsymbol{\Sigma}_{y'}^{-1}} + ||\boldsymbol{d}_k-\boldsymbol{\mu}_{d_k}||^2_{\boldsymbol{\Sigma}_{d_k}^{-1}}). \quad \text{(25b)}$$

measurements to the new measurement vector $\boldsymbol{y}''$ denotes as,

$$\boldsymbol{y}'' = \left[({}^m\boldsymbol{a}_0^g)^\top \quad \dots \quad ({}^m\boldsymbol{a}_{N_s}^g)^\top \quad (\widehat{\boldsymbol{f}}_0^x)^\top \quad \dots \quad (\widehat{\boldsymbol{f}}_{N_{B-1}}^x)^\top\right]^\top. \quad (24)$$

An updated dynamics estimation problem with the new measurement vector $\boldsymbol{y}''$ is considered as the second step. It is important to notice that the measurement covariances for the first step $\boldsymbol{\Sigma}_{y'}$ and the second step $\boldsymbol{\Sigma}_y$ are independent and different parameters.

IV. VALIDATION

A. EXPERIMENTAL SETUP

The validation of the presented approach of non-collocated wrench estimation is carried through experiments with human subjects using two different types of measurement systems. The first measurement system is related to human motion tracking and we use Xsens inertial motion tracking system which consists of 17 distributed inertial measurement units (IMUs) placed at different body parts of the subject. We obtain the pose, velocity, and acceleration measurements of different body segments that constitute the links of our human model as shown in Fig. 3. This information is used to compute the joint position and velocity which constitutes the internal state information through dynamical inverse kinematics [40]. It is important to highlight that in this work the human pose estimation i.e., inverse kinematics is not formulated as a stochastic estimation problem. Hence, the human joint quantities such as positions and velocities are not dependent on any measurement covariance values. However, we thoroughly demonstrate and validate the approach of non-collocated wrench estimation in experimental scenarios involving different motions that are composed of various human pose configurations as described in Section IV-B.

The rigid-body human model[1] is constructed through anthropometric tables using subject-specific measurements and is composed of 23 link segments with each pair of links connected through three one degree of freedom rotational joints. Although it is evident that the modeling assumption of the human body as an articulated rigid body system is quite limited in terms of capturing the complexity of a sophisticated musculoskeletal structure, it is a necessary assumption

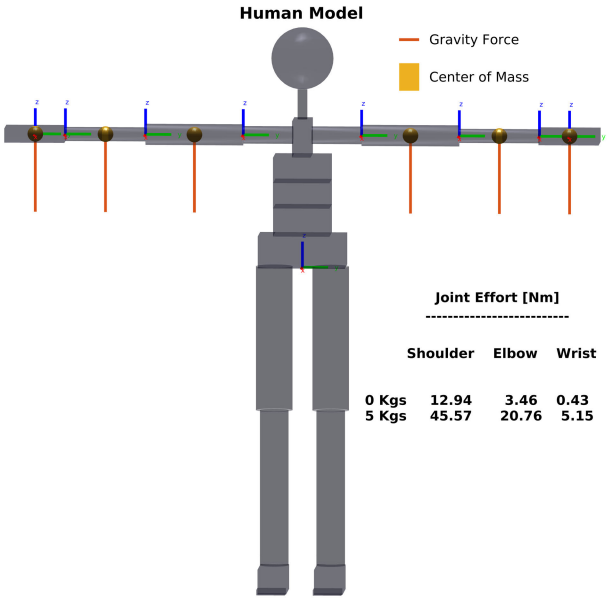

FIGURE 3. Human model in *Tpose* configuration with frame locations of the shoulder, elbow, and wrist joints along with the center of mass (CoM) locations of the upper arm, forearm, and hand links. Also, the frame located at the center of mass of the hand link is highlighted. Baseline joint effort values are computed for an ideal *Tpose* configuration where the joint's position, velocity, and acceleration values are set to 0. The resulting joint effort corresponds to the gravity compensation torque. Two cases of no-load (0 kg) and load (5 kg) at the center of mass frame of the hand link are considered, and the resulting joint effort experienced due to gravitational force is computed. Note that the joint effort values displayed in the figure are absolute values.

considered towards building the framework towards enabling novel HRC scenarios [15], [27].

The second type of measurement system provides the wrench measurement at the feet of the human subject. We consider two different types of wrench measurement systems. The first wrench measurement system is ground fixed AMTI force plates,[2] which are a widely used standard wrench measurement system for biomechanical studies. This choice is made to demonstrate the validation experiments using an industry-standard as the equipment for ground reaction force-torque measurements. The second wrench measurement system is a wearable technology that is a pair of sensorized shoes developed at the Italian Institute of

[1] https://github.com/robotology/human-gazebo

[2] https://amti.biz/fps-guide.aspx

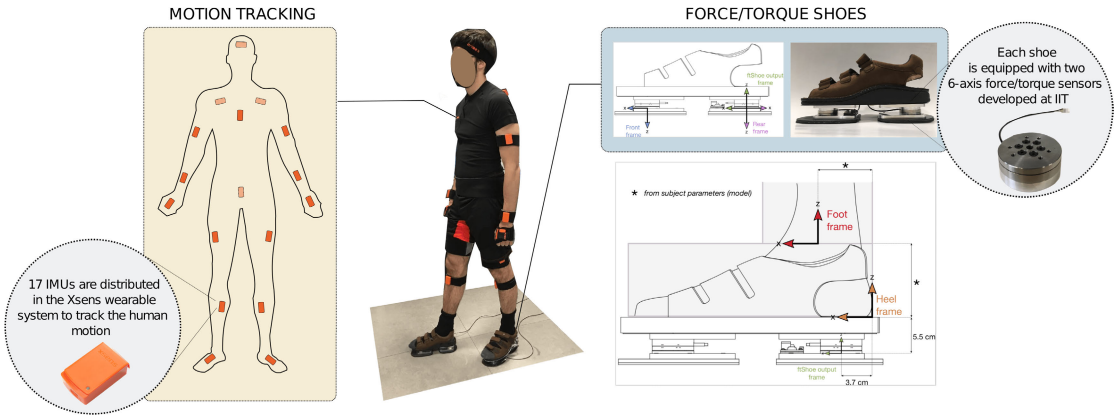

FIGURE 4. Subject wears Xsens inertial motion tracking system and a pair of sensorized shoes equipped with force/torque sensors developed at IIT.

Technology[3] (IIT). Each shoe is equipped with two Force/Torque sensors, one at the front of the shoe and the other at the back. The wrench measurements coming from different measurement systems are expressed in the frame associated with the human foot link. The various measurement systems used in the experiments are shown in Fig. 4 and Fig. (5a).

B. EXPERIMENTAL SCENARIOS

We considered two different experimental scenarios, with two different subjects. The first experimental scenario is referred to as the *validation scenario*. For this scenario we considered ground fixed AMTI force plates as the source of wrench measurements. The validation scenario constitutes of two experiments where 1) the subject standing in *Npose* configuration (Fig. (5a)) moves both the arms to a *Tpose* configuration (Fig. (5b)) without any load at the hands, and 2) the subject standing in *Npose* configuration moves the right (dominant arm) to a *Tpose* configuration with a 5 kg payload (Fig. 5c)).

The second experimental scenario is referred to as the *application scenario* where a real-world application of carrying a heavy payload with both hands is considered and the proposed non-collocated wrench estimation approach is used to estimate the mass of the object. The sensorized shoes are considered as the source of wrench measurement. Unlike the ground fixed plates, sensorized shoes facilitate the mobility of the subject to perform dynamic motions like walking. The application scenario constitutes two sets of experiments. The first set of experiments conducted are based on quasi-static human motion as highlighted in Fig. 6. The subject initially stands in a static neutral *Npose* (6a), moves forward, and picks up the payload placed in front of him (6b), balances on his left foot (6c), then the right foot (6d) while holding the payload with his hands. The second set of experiments involves a dynamic motion while the human carries the payload as highlighted in Fig. 7. The subject initially stands in a static neutral *Npose* (7a), moves forward and picks up the payload placed in front of him (7b), and walks a few steps while carrying the payload. Particular instances when the left foot (7c) and the right foot (7d) are in contact with the ground during the dynamic walking motion are shown.

Heterogeneous experimental data coming from Xsens inertial motion tracking system, AMTI force plates and the sensorized Force/Torque shoes are combined into a

[3]https://dic.iit.it/

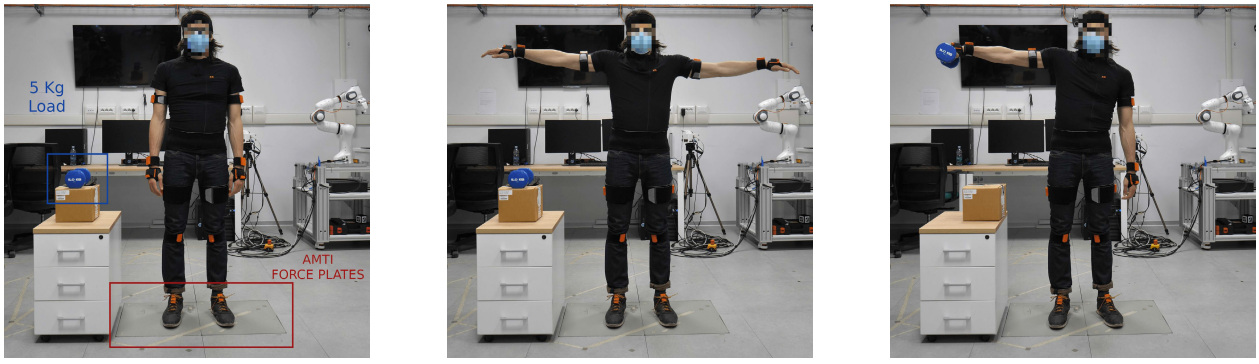

FIGURE 5. Validation scenario experiments showing instances of a subject in a) Npose configuration, b) Tpose configuration of both the arms, and c) Tpose configuration of the dominant right arm with 5 kg payload. During both the validation scenarios the subject is initially in the Npose configuration, moving the Tpose configuration with both the arms or the dominant right arm with 5 kg payload, and moves back to Npose configuration.

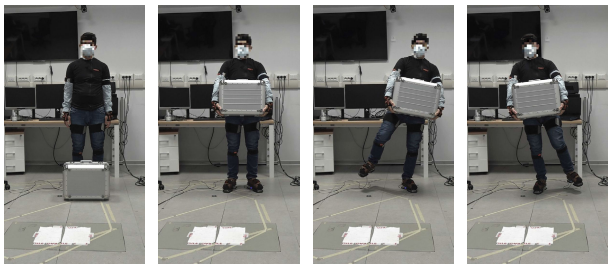

(a) (b) (c) (d)

FIGURE 6. Application scenario experiment showing instances of a) Npose without payload, b) Npose with payload, c) left foot balancing with payload, and d) right foot balancing with payload during quasi-static human motion.

(a) (b) (c) (d)

FIGURE 7. Application scenario experiment showing different instances of a) Npose without payload, b) Npose with payload, c) walking instance with left foot in contact, and d) walking instance with right foot in contact during dynamic human motion.

homogeneous ''wearable'' data format through the use of wearables library,[4] that is logged at a frequency of 50 Hz through YARP middleware [46]. The logged homogeneous data is played back in real-time to run the stochastic inverse dynamics algorithm[5] ''without'' and ''with'' the non-collocated wrench estimation approach. To be more precise, the case of without non-collocated wrench estimation refers to the old approach of stochastic inverse dynamics explained in Section II-B, while the case of with non-collocated wrench estimation refers to the approach presented in Section III-A. The estimates of the dynamic variables are saved in Matlab data format for plotting the results presented in the next section.

C. RESULTS AND DISCUSSION

The validation scenario experiments are used to demonstrate the estimation of feet and hands external link wench estimation for different choices of measurement covariances. Also, it is used for the validation of joint torques estimation using the original stochastic inverse dynamics approach presented in Section II-B. More importantly, the limitation of the original stochastic inverse dynamics approach for external interaction wrench estimation presented in Section II-C is highlighted quantitatively, and the utility of the proposed approach of non-collocated wrench estimation (NCWE) presented in Section III-A is demonstrated. Later, the experimental results of the application scenario highlight the utility of the non-collocated wrench estimation approach for practical real-world scenarios tasks such as carrying a heavy payload. As we consider a rigid body human model, the exact *frame* that is considered to be the contact location for the wrench estimation is at the Center of Mass of the hand link as shown in Fig. (3). Note that any further references to the hand link correspond to the link that is defined at the Center of Mass of the hand link.

All the wrench quantities presented in this section are expressed in the inertial frame of reference. The force components are denoted as f_x, f_y, f_z, and the moment/torque components are denoted as m_x, m_y, m_z. The start and the end instances of Tpose configuration during the validation scenario are indicated with vertical dashed lines. The covariance values chosen for different experimental scenarios are highlighted in Table 1. Note that the main motivation behind choosing different covariance values for different experimental scenarios is to demonstrate the limitation of the original stochastic inverse dynamics approach, and to highlight the utility of non-collocated wrench estimation and associated joint torque estimation under the influence of a payload. To utilize the proposed approach for real-world applications, the covariance values indicated in Table 1 under the application scenario experiments are used.

1) Tpose WITHOUT LOAD

The effect of measurement covariance values is previously discussed in Section II-B4. The experiments of the validation scenario have the measurement forces and torques at the feet coming from the AMTI force plates. Fig. 8 highlights the error between the measurements and the feet external wrench estimates for different measurement covariance values. The choice of a small value such as 10^{-6} indicates our trust in the wrench measurement values that leads to a small error when compared against other choices of the feet wrench measurement covariance. So, the choice of 10^{-6} leads to the estimated feet wrench to be close to the measurements from AMTI force plates as highlighted in Fig. 9. The weight of the subject is around 75.5 kg during the time of the experiment. The wrench indicated here is expressed with respect to the inertial frame of reference. So, the variation of the measured wrench indicated here results from two possible sources of error: a) the measurement accuracy ($\pm 0.5\%$ of applied load) of the force plates, and b) the possible errors in kinematics information resulted from the inverse kinematics solution. However, looking at the force components, only the force component along the z-axis is prominent and is close to the gravity wrench under the influence of the subject weight. Whereas the force components along the x-axis and y-axis are small. Concerning the moment components, the values indicated are a direct result of the consideration of moments in the inertial frame of reference. Note that the close match between the measurements and the estimates is a direct indication of

[4]https://github.com/robotology/wearables
[5]https://github.com/robotology/human-dynamics-estimation

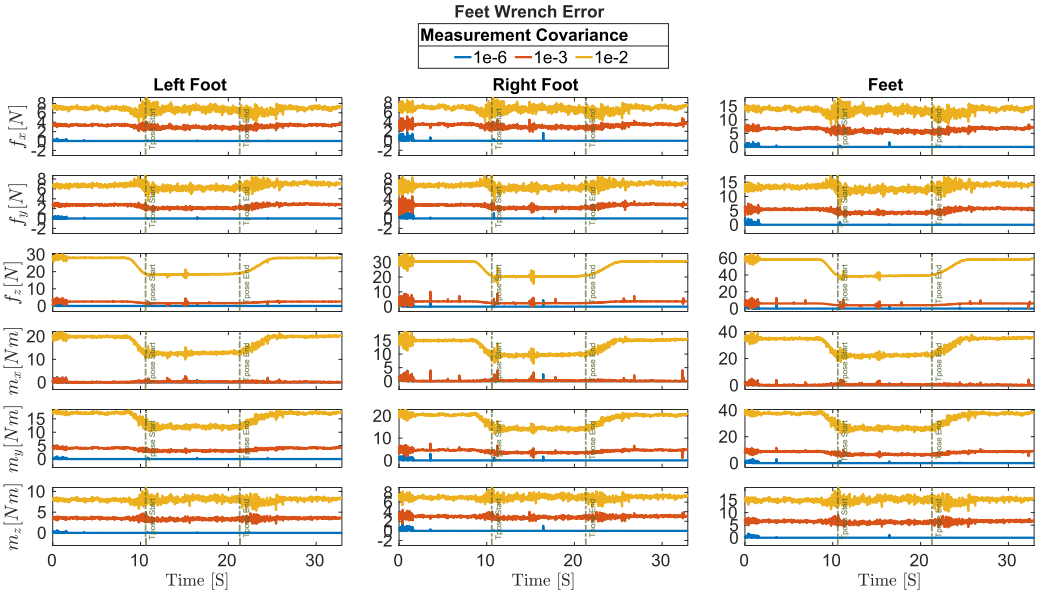

FIGURE 8. Feet wrench error between the measurements from AMTI force plates and the estimates for different feet measurement covariance values during Tpose without load validation scenario experiment shown in Fig. (5b). An increase in feet wrench measurement covariance increases the error indicating the feet wrench estimates diverge from the measurements from AMTI force plates. Following the discussion of covariance tuning explained in Section II-B4, choice of wrench measurement covariance value 10^{-6} results in the feet wrench estimates close to the measurements from AMTI force plates. The start and end of the Tpose configuration is highlighted with vertical dashed lines.

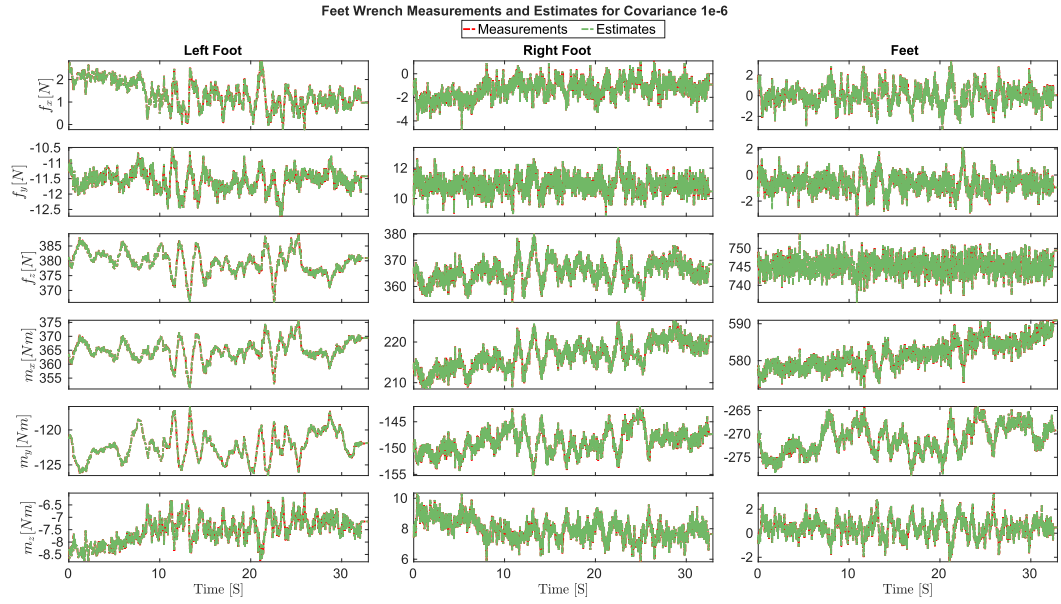

FIGURE 9. Feet wrench tracking between the measurements and the estimates for feet wrench measurement covariance value of 10^{-6} during Tpose without load validation scenario experiment shown in Fig. (5b). The weight of the subject is around 75.5 kg during the time of the experiment. The wrench indicated here is expressed with respect to the inertial frame of reference. So, the variation of the measured wrench indicated here results from two possible sources of error: a) the measurement accuracy (±0.5% of applied load) of the force plates, and b) the possible errors in kinematics information resulted from the inverse kinematics solution. However, looking at the force components, only the force component along the z-axis is prominent and is close to the gravity wrench under the influence of the subject weight. Whereas the force components along the x-axis and y-axis are small. Concerning the moment components, the values indicated are a direct result of the consideration of moments in the inertial frame of reference. Note that the close match between the measurements and the estimates is a direct indication of the accuracy of the estimation that resulted from choosing a small measurement covariance value of 10^{-6}.

the accuracy of the estimation that resulted from choosing a small measurement covariance value of 10^{-6}.

The joint torque estimates at shoulder, elbow, and wrist joints using feet wrench measurement covariance value

of 10^{-6} are shown in Fig. 10. The joint effort is computed as the L2 norm of the corresponding three one DoF joints between the two link segments of the human model. Following (23), the estimation of joint torques depends on the model covariance $\mathbf{\Sigma}_D$ that is set to a value of 10^{-6} to ensure all the model constraints are respected. During the Tpose configuration, the estimated joint effort is around the baseline joint effort that is shown in Fig. 3. The baseline joint effort is computed by manually setting the joint position, velocity, and acceleration values to zero for the human model which results in an ideal Tpose configuration. So, the resulting baseline joint effort corresponds to the gravity compensation torques for the upper arm, forearm, and hand of the subject during the Tpose configuration. The human subject cannot assume an ideal Tpose configuration and this results in joint effort estimates that are different from the exact baseline joint effort values. Additionally, the joint torque estimates are compared against *computed torques* that are computed through deterministic inverse dynamics using the joint position, velocity, acceleration, and the external interaction wrench measurements at the feet from the experiment. Computed torques are obtained using iDynTree[6] library [31]. It is important to highlight that this validation of joint torque estimation and the resulting joint effort with respect to the baseline joint efforts and computed torques complements the original validation results presented in [24].

[6]https://github.com/robotology/idyntree

2) Tpose WITH LOAD

Concerning the experiment where the subject moves the dominant right arm from Npose to Tpose configuration with a 5 kg payload, we are certain that no external interaction wrench is present on the left hand of the subject. Hence, we consider zero wrench measurement and a low measurement covariance value of 10^{-6} for the left hand. This results in the left hand wrench estimates to be close to its set zero measurement, i.e., $\mathbf{0}_{6\times1}$ which is evident from the results highlighted in Fig. 11 and Fig. 13.

Now, the link that is considered for wrench estimation is at the Center of Mass of the right-hand link. During this validation experiment, it is clear that the external force acting on the link is the gravitational force of the payload, and the moments generated at the considered frame are small. So, we consider a high measurement covariance value of 10^4 for the moments at the right hand Center of Mass link. Wrench estimation for different force measurement covariances without the consideration of non-collocated wrench estimation is highlighted in Fig. 11. The increase in measurement covariance results in higher values of the wrench estimates. However, the resulting estimates do no reflect the payload that is being held by the subject. This is evident from the estimated object mass results highlighted in Fig. 12. The object mass is computed through the L2 norm of the estimated right-hand forces. These results demonstrate the limitation of the original approach of stochastic human inverse dynamics presented in Section II-C.

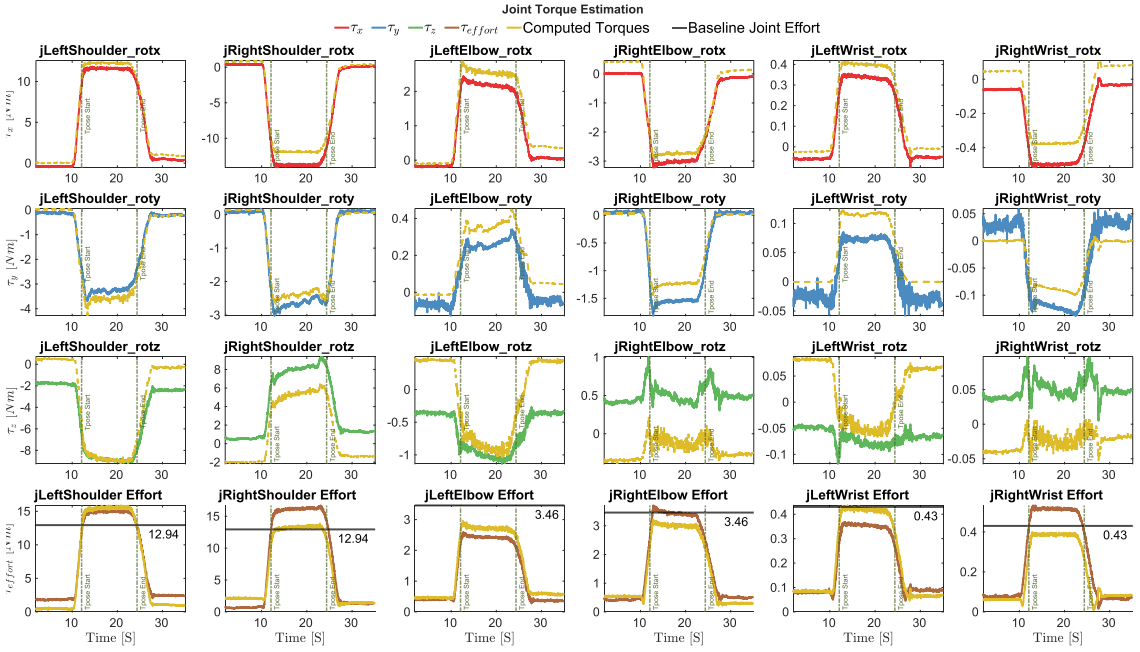

FIGURE 10. Torque estimates for shoulder, elbow, and wrist joints during Tpose without load validation scenario experiment shown in Fig. (5b) using feet wrench measurement covariance value of 10^{-6}. The name of the joint of the human model is indicated in the title of the subplots. The subject stands in Npose configuration, moves to Tpose configuration, and moves back to Npose configuration. The start and end of the Tpose configuration are highlighted with vertical dashed lines. Computed torques indicate the joint torques computed through deterministic inverse dynamics using the joint position, velocity, acceleration, and the external interaction wrench measurements at the feet from the experiment.

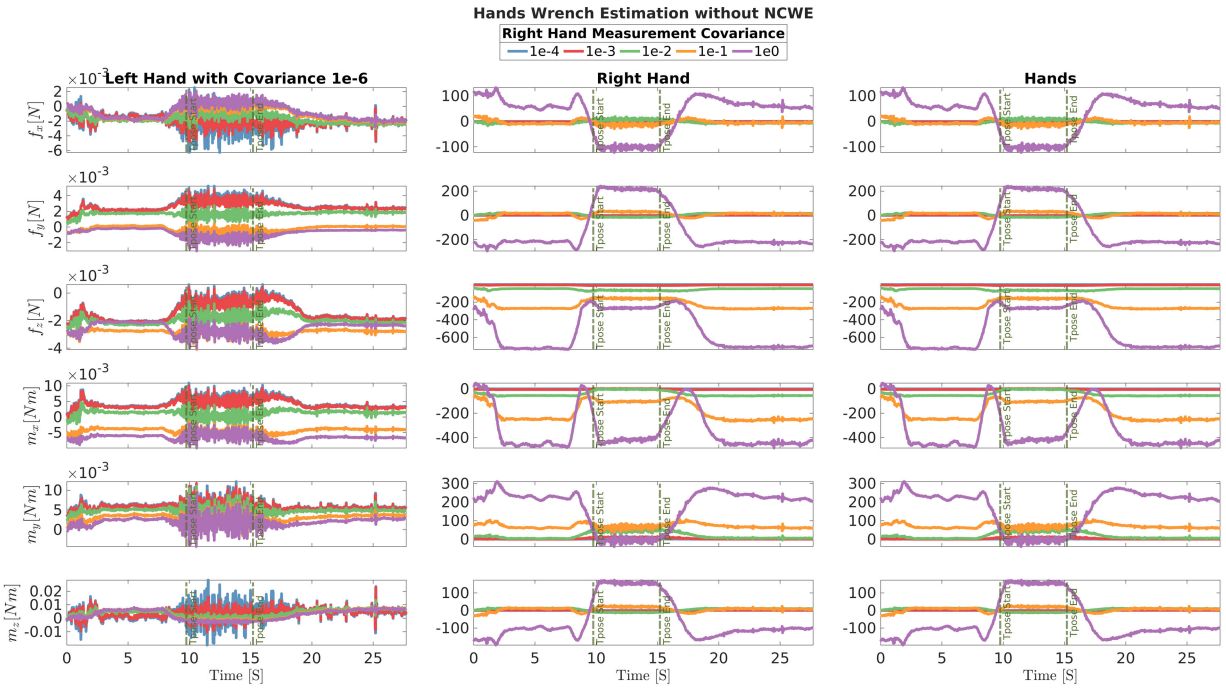

FIGURE 11. Hands wrench estimation without non-collocated wrench estimation for different measurement covariance values during the 5 kg payload validation experiment shown in Fig. (5c). The subject stands in Npose configuration, moves to pick up a 5 kg payload, lifts the right hand to Tpose configuration, and moves back to Npose configuration. The start and end of the right-hand Tpose configuration are highlighted with vertical dashed lines. Left hand wrench measurement covariance value is set to 10^{-6} as there is no payload, and the resulting wrench estimates are close to the set zero measurements. Right hand wrench estimates increase with increasing measurement covariance value. However, the resulting wrench estimates do not reflect the wrench experienced under the influence of 5 kg payload.

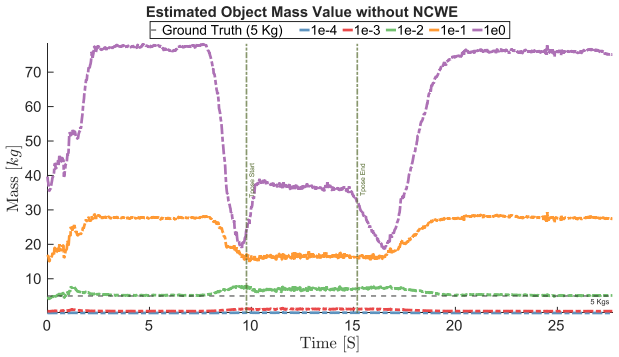

FIGURE 12. Object mass estimation without non-collocated wrench estimation for different measurement covariance values during the 5 kg payload validation experiment shown in Fig. (5c). The start and end of the right-hand Tpose configuration are highlighted with vertical dashed lines. Object mass is computed as the L2 norm of the estimated hand wrenches highlighted in Fig. 11. The estimated object mass does not reflect the 5 kg payload held by the subject.

On the other hand, using the approach of non-collocated wrench estimation results in right hand wrench estimates that are physically consistent with the 5 kg payload that is held by the subject. This is evident from the wrench estimation presented in Fig. 13, and the resulting payload mass estimation shown in Fig. 14. One key detail that needs to be highlighted here is the measurement covariance values for the rate of change of momentum from (14). As it is composed of link velocity and acceleration values that can be noisy, a value of 10^{-3} is chosen. So, a measurement covariance value of 10^{-4} for the right-hand wrench does not result in any estimates greater than their set zero measurements. Whereas, choosing values greater than 10^{-3} starts yielding wrench estimates that are physically consistent with the 5 kg payload held by the subject in the right hand.

RViz 3D visualization of payload mass estimation without and with non-collocated wrench estimation for different measurement covariance values is indicated in Fig. 15. Using the original stochastic inverse dynamics approach, i.e., without the non-collocated wrench estimation, the estimated object mass value is inconsistent with respect to the 5 kg payload held by the subject. On the other hand, the proposed non-collocated wrench estimation approach results in an estimated object mass that is consistent with the 5 kg payload held by the subject at the right hand.

The joint torque estimates and the joint effort values for the shoulder, elbow, and wrist joints during the Tpose configuration under the influence of the 5 kg payload at the right hand is shown in Fig. 16. Consideration of non-collocated wrench estimation directly results in the joint effort values that are around the baseline values shown in Fig. 3 for the case of 5 kg payload.

3) APPLICATION SCENARIO

The ground truth mass of the payload handled by the human during the application scenario is 9.55 kg. In this scenario,

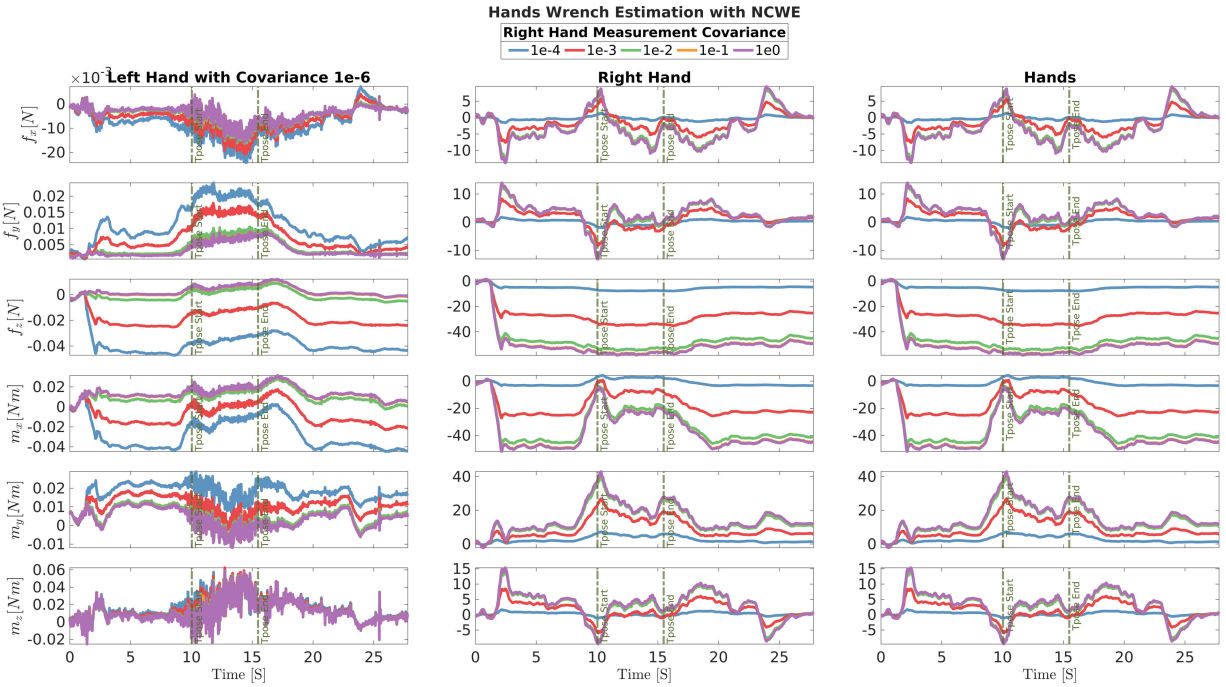

FIGURE 13. Hands wrench estimation with non-collocated wrench estimation for different measurement covariance values during the 5 kg payload validation experiment shown in Fig. (5c). The subject stands in Npose configuration, moves to pick up a 5 kg payload, lifts the right hand to Tpose configuration, and moves back to Npose configuration. The start and end of the right-hand Tpose configuration are highlighted with vertical dashed lines. Left hand wrench measurement covariance value is set to 10^{-6} as there is no payload, and the resulting wrench estimates are close to the set zero measurements. Right hand wrench estimates increase with increasing measurement covariance value, and the resulting wrench estimates reflect the wrench experienced under the influence of 5 kg payload.

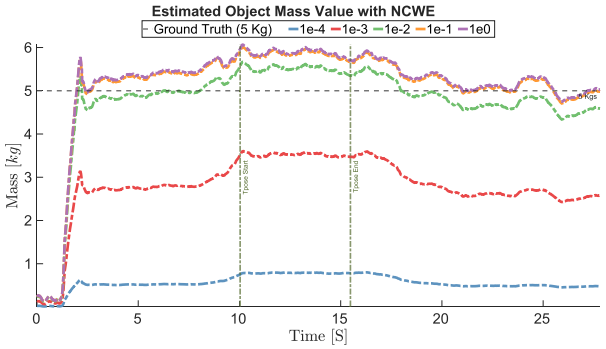

FIGURE 14. Object mass estimation with non-collocated wrench estimation for different measurement covariance values during the 5 kg payload validation experiment shown in Fig. (5c). The start and end of the right-hand Tpose configuration are highlighted with vertical dashed lines. Object mass is computed as the L2 norm of the estimated hand wrenches highlighted in Fig. 13. The estimated object mass reflects the 5 kg payload held by the subject.

the subject holds and carries the payload using both arms. So, following the discussion presented in Section IV-C2, the wrench measurement covariance values of both the left hand and the right hand are set as to estimate forces and moments experienced under the influence of the payload. Non-collocated wrench estimation results corresponding to the quasi-static human motion experiment depicted in Fig. 6 are shown in Fig. 17, while the results corresponding to the dynamic human motion experiment depicted in Fig. 7 are shown in Fig. 18. As explained in section III-A, the measurement value of each of the wrench components is set zero, i.e., $\mathbf{0}_{6\times1}$. Considering our approach of non-collocated wrench estimation through centroidal dynamics constraint, the external force estimates at the hands are guided to reflect the weight of the payload handled by the subject. It is important to observe that the centroidal dynamics constraint is composed of six dimensions. So, one of the limitations of the proposed approach to situations like the application scenario is that only three components of forces or three components of torques can be estimated individually. This limits the possibility to control the estimation of forces or torques at both hands simultaneously.

The mass of the object is computed as the L2 norm of the increased force measurements at the feet under the influence of the object, and the L2 norm of the force estimates at the hands is highlighted in the last row of Fig. 17 and Fig. 18. After the initial neutral Npose, the subject moves down to pick up the object, and this is a transient phase where the feet contact with the ground is unstable along with a significant change in the body posture. This is visible through the transient phase indicated by the vertical lines. Following this transient phase, the estimation of the object mass is close to the ground truth mass of 9.55 kg, even during the contact transitions of the feet during the dynamic walking motion.

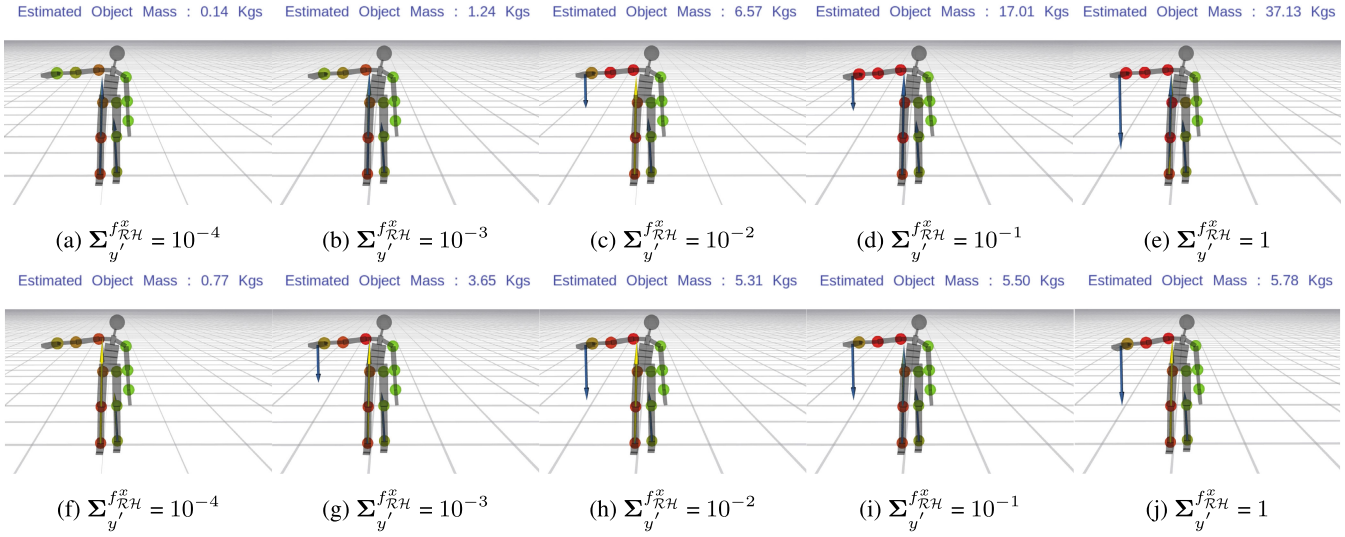

FIGURE 15. RViz 3D visualization of 5 kg payload mass estimation during right hand Tpose configuration (15a)-(15e) without non-collocated wrench estimation, and (15f)-(15j) with non-collocated wrench estimation for different measurement covariance values for the right hand forces, i.e., $\Sigma_{y'}^{f_{\mathcal{RH}}^{x}}$. The estimated object mass does not reflect the 5 kg payload as highlighted in Fig. 12. The blue arrow at the hand is a representative indication of the estimated hand force, but the scale does not correspond to the magnitude of the estimated forces. The yellow arrow at the feet represents the ground reaction force that is measured and the blue line represents the estimated force at the feet links. Using the feet wrench measurement covariance value of 10^{-6}, the force estimates are similar to the force measurements at the feet. The spheres indicated the joint effort, with green color representing a low joint effort value and the color red representing a high joint effort value.

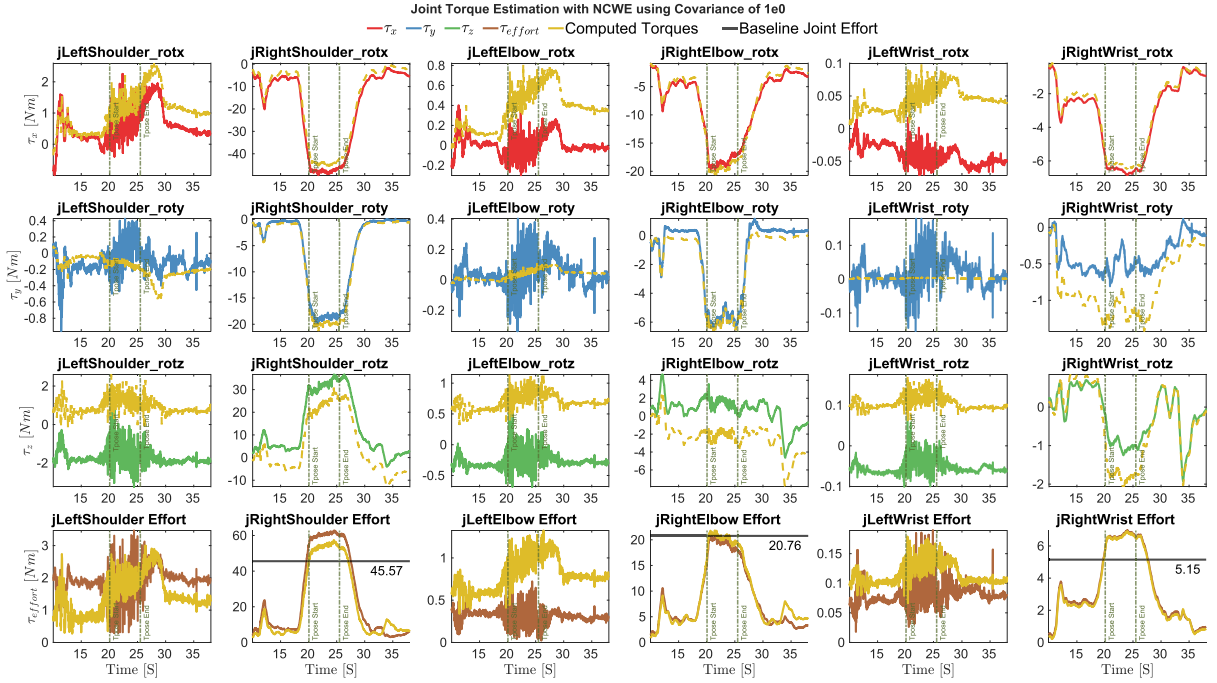

FIGURE 16. Torque estimates for shoulder, elbow, and wrist joints using non-collocated wrench estimation with right hand force measurement covariance value of 1 during Tpose with 5 kg payload validation scenario experiment shown in Fig. (5c). The name of the joint of the human model is indicated in the title of the subplots. The subject stands in Npose configuration, moves to pick up a 5 kg payload, lifts the right hand to Tpose configuration with the payload, and moves back to Npose configuration. Estimated joint torques and effort are closer to the joint torques and effort computed through deterministic inverse dynamics. The start and end of the right-hand Tpose configuration are highlighted with vertical dashed lines. Computed torques indicate the joint torques computed through deterministic inverse dynamics using the joint position, velocity, acceleration, and the external interaction wrench measurements at the feet from the experiment.

Fig. 19 highlights visualization of the estimated wrench at the hands and the joint effort estimated during different instances of the task. While the subject is standing in neutral *Npose* without any object at the hands, the estimated wrench at the hands is close to zero and the upper body joints do not experience any effort as shown in Fig. (19a).

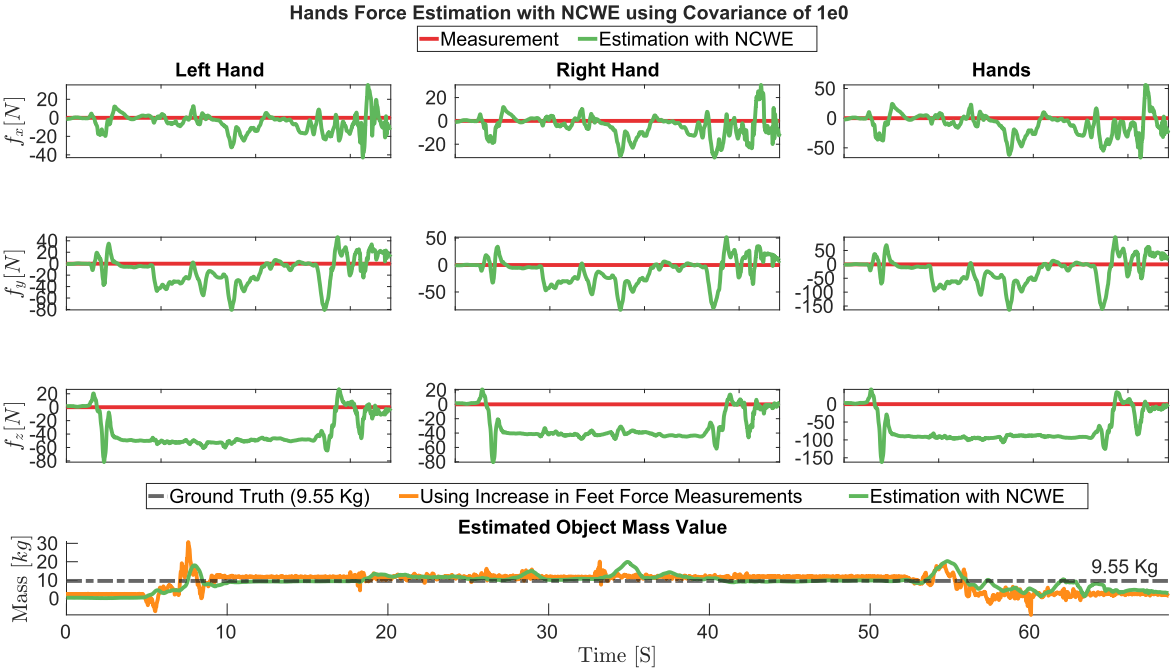

FIGURE 17. Application of non-collocated wrench estimation during quasi-static motion from experiments highlighted in Fig. 6. As the subject handles the payload with both the arms, the wrench measurement covariance at both the right hand and left hand is set to a value of 1. Force estimation at both the left and the right hand is highlighted to emphasize the utility of the non-collocated wrench estimation approach in estimating the interaction force experienced under the influence of the payload. The force measurement at the hands is set zero, i.e., $0_{3\times1}$. Furthermore, payload mass estimation during quasi-static human motion is presented in comparison with the mass computed as the L2 norm of the increase in force measurements at the feet.

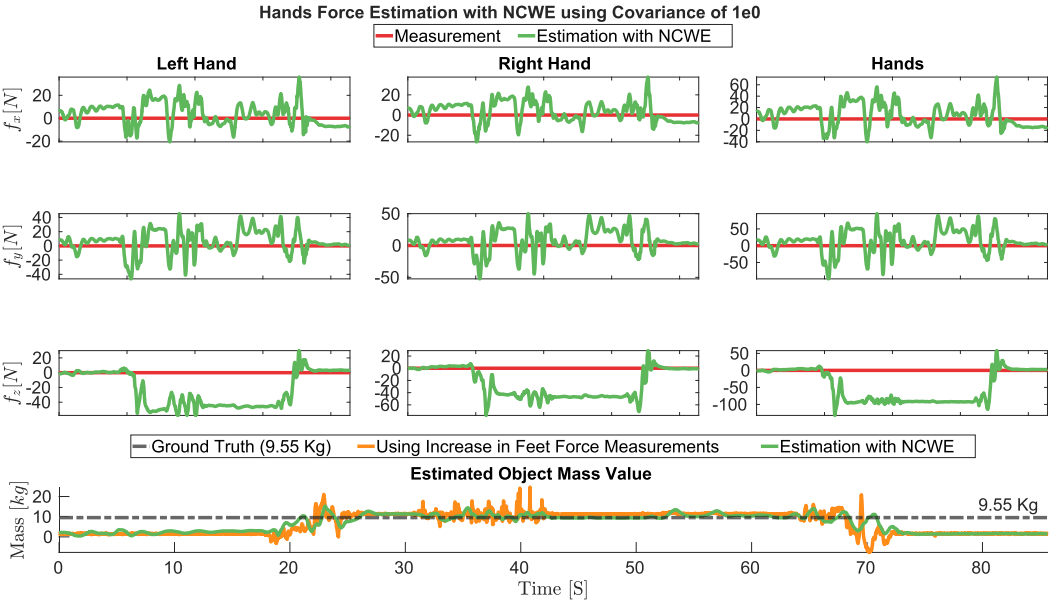

FIGURE 18. Application of non-collocated wrench estimation during dynamic walking motion from experiments highlighted in Fig. 7. As the subject handles the payload with both the arms, the wrench measurement covariance at both the right hand and left hand is set to a value of 1. Force estimation at both the left and the right hand is highlighted to emphasize the utility of the non-collocated wrench estimation approach in estimating the interaction force experienced under the influence of the payload. The force measurement at the hands is set zero, i.e., $0_{3\times1}$. Furthermore, payload mass estimation during quasi-static human motion is presented in comparison with the mass computed as the L2 norm of the increase in force measurements at the feet.

On the other hand, when the subject is holding the object the estimated wrench at the hands is highlighted through blue arrows, and the joints in the upper body experience effort as shown in Fig. (19b). While the subject is walking, depending on the foot that is in contact, either the left leg as shown in Fig. (19c), or the right leg as shown in Fig. (19d) experiences higher effort, while the estimated wrench at the hands is consistent as highlighted through the

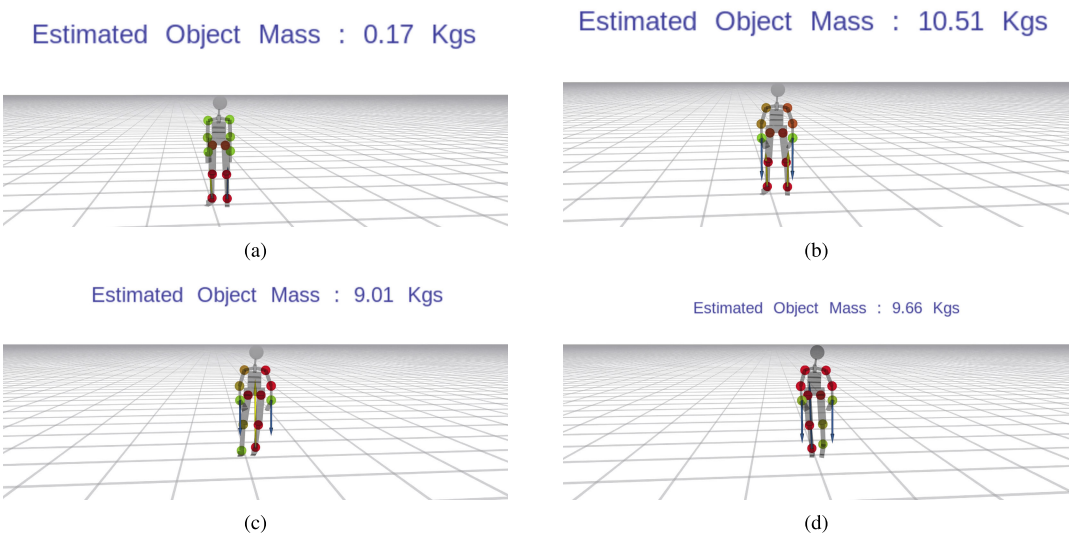

FIGURE 19. RViz 3D visualization for application scenario of walking with non-collocated wrench estimation while carrying a payload of 9.55 kg. The blue arrows at the hands are a representative indication of the estimated hand forces, but the scale does not correspond to the magnitude of the estimated forces.

estimated object mass value that is close to the ground truth of 9.55 kg.

V. CONCLUSION AND REMARKS

Real-time assessment of human ergonomic indices is receiving attention with the development of novel tools and techniques. An interesting open problem we consider in this work is to estimate the external interaction wrench experienced at human extremities such as hands while carrying heavy objects. We highlighted the current limitations of the stochastic human inverse dynamics approach in the literature, and propose an updated formulation through the consideration of centroidal dynamics constraint. We highlighted the effect of different choices of measurement covariance values using a validation experimental scenario and demonstrated the usefulness of the proposed non-collocated wrench estimation approach in terms of estimating the external interaction wrench experienced at the hands, along with the corresponding joint torque estimation. Furthermore, we present the benefit of non-collocated wrench estimation for a real-world application scenario of carrying a heavy object that involved dynamic human motion such as walking.

At this stage, it is important to point out some of the limitations and challenges in applying our proposed approach in real industrial environments. One of the key limiting technologies is the current version of the sensorized shoe that severely limits the natural gait of the subject. Restrictions of motion of any sort that are caused due to the wearability of a system is a key challenge to overcome in realizing many potential applications for the industrial sector using wearable technology [47]. So, improvements in the direction of wearability through the usage of lightweight materials such as Graphene and wireless connectivity for data acquisition are some of the key technical activities that enable the use of sensorized shoes in a wide variety of practical applications such as industrial environments and rehabilitation. At the modeling level, musculoskeletal modeling of humans lead to novel research investigations. Also, consideration of contact localization through human action recognition can enhance the applicability of the proposed approach to a wide variety of scenarios. Technically, our approach is straightforward to set up in real-world environments, as long as the different sensory measurements, and modeling tools are available. However, the system complexity arises primarily from the consideration of heterogeneous measurement systems such as the motion tracking system and the force-torque measurement systems explained in Section IV-A. Such measurement systems are often available from different commercial vendors who specialize in a single measurement system, and establishing a robust software infrastructure to integrate different measurement systems is often a daunting task. This work is realized using a variety of open-source software tools for modeling,[7] heterogeneous measurement data serialization,[8] and estimation algorithms[9] [10] that can be set up easily through a meta-repository.[11] A key technical challenge is to realize a single wearable system that combines different measurement modalities[12] and provides a quick and easy-to-use software infrastructure. Furthermore, adding feedback infrastructure such as haptic actuation will open novel applications in the field of real-time ergonomy assessment and assistance for the future socio-technical workforce.

This manuscript primarily aims at presenting and thoroughly validating the approach of non-collocated wrench estimation and the joint torque estimation for real-time

[7] https://github.com/robotology/human-gazebo
[8] https://github.com/robotology/wearables
[9] https://github.com/robotology/idyntree
[10] https://github.com/robotology/human-dynamics-estimation
[11] https://github.com/robotology/robotology-superbuild
[12] https://ifeeltech.eu/

TABLE 1. Table indicating the different covariance values chosen for the experiments presented in Section IV. Note that the main motivation behind the different covariance values chosen for different experimental scenarios is to demonstrate the limitation of the original stochastic inverse dynamics approach and to highlight the utility of non-collocated wrench estimation and the associate joint torque estimation under the influence of a payload. To utilize the proposed approach for real-world applications, the covariance values indicated under the application scenario experiments are used.

Covariance Values			
Covariance Type	Validation Scenario		Application Scenario
	Tpose **without** Load	Tpose **with** Load	
$\mathbf{\Sigma}_d$	10^6	10^6	10^6
$\mathbf{\Sigma}_D$	10^{-6}	10^{-6}	10^{-6}
$\mathbf{\Sigma}_{y'}$ Feet	-	10^{-6}	10^{-6}
$\mathbf{\Sigma}_{y'}$ Hand Forces	-	1	1
$\mathbf{\Sigma}_{y'}$ Hand Moments	-	10^{-4}	1
$\mathbf{\Sigma}_y$ Feet	10^{-6}	10^{-6}	10^{-6}
$\mathbf{\Sigma}_y$ Hands	10^{-6}	10^{-6}	10^{-6}

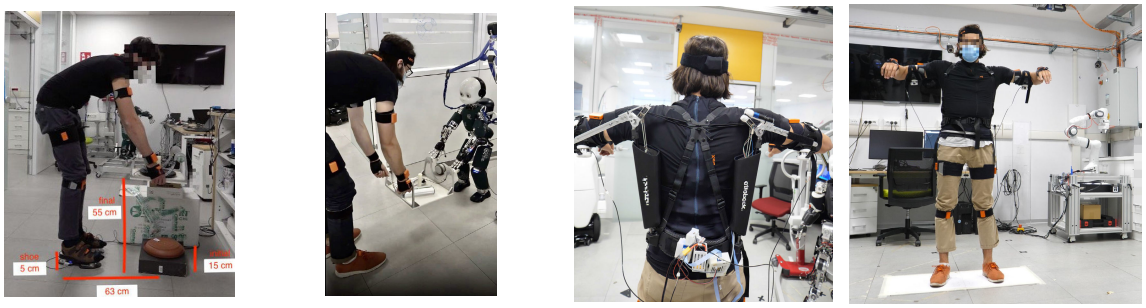

(a) (b) (c) (d)

FIGURE 20. Experiments highlighting future research investigations in a) real-time risk classification during material handling, b) human-robot collaborative object co-manipulation and transport, c) an active exoskeleton that provides support during overhead tasks, and d) a human subject wearing an active exoskeleton that provides support during overhead tasks with human-in-the-loop adaptive control strategies. All of these future research directions leverage the approach of non-collocated wrench estimation for real-time estimation of interaction wrench under the influence of a payload at contact locations that do not have direct sensor measurements.

assessment of human ergonomic indices. We consider non-collocated wrench estimation to be a fundamental enabling technique that facilitates future research investigations involving real-time risk classification during material handling in logistics [48], [49], partner-aware whole-body humanoid control in providing assistance during Human-Robot Collaboration tasks such as collaborative object co-manipulation and transport [20], [27], and control of adaptive exoskeletons for evaluating and validating the amount of support they provide for overhead tasks on the shop floor [14], [15], [21].

Some future research investigations are highlighted in Fig. 20 showing experiments related to real-time risk classification during material handling Fig. (20a), human-robot collaborative object co-manipulation and transport Fig. (20b), an active exoskeleton that provides support during overhead tasks with human-in-the-loop adaptive control strategies Fig. (20c)-(20d). All of these future research directions leverage the approach of non-collocated wrench estimation for real-time estimation of interaction wrench under the influence of a payload at contact locations that do not have direct sensor measurements.

ACKNOWLEDGMENT

The authors would like to sincerely thank Dr. Vishal Ramadoss for his thorough review of this manuscript.

REFERENCES

[1] S. Pfeiffer, "Robots, industry 4.0 and humans, or why assembly work is more than routine work," *Societies*, vol. 6, no. 2, p. 16, May 2016.
[2] D. P. Valentina, D. S. Valentina, M. Salvatore, and R. Stefano, "Smart operators: How industry 4.0 is affecting the worker's performance in manufacturing contexts," *Procedia Comput. Sci.*, vol. 180, pp. 958–967, Jan. 2021.
[3] E. Laudante, "Industry 4.0, innovation and design. A new approach for ergonomic analysis in manufacturing system," *Des. J.*, vol. 20, no. 1, pp. S2724–S2734, Jul. 2017.
[4] P. Kuhlang, M. Ostermeier, and M. Benter, "Human work design: Modern approaches for designing ergonomic and productive work in times of digital transformation—An international perspective," in *Proc. 20th Congr. Int. Ergonom. Assoc. (IEA)*, S. Bagnara, R. Tartaglia, S. Albolino, T. Alexander, and Y. Fujita, Eds. Cham, Switzerland: Springer, 2019, pp. 29–37.
[5] Y. Lu, J. S. Adrados, S. S. Chand, and L. Wang, "Humans are not machines—Anthropocentric human–machine symbiosis for ultra-flexible smart manufacturing," *Engineering*, vol. 7, no. 6, pp. 734–737, Jun. 2021. [Online]. Available: https://www.sciencedirect.com/science/article/pii/S2095809921001612
[6] E. E. Broday, "Participatory ergonomics in the context of industry 4.0: A literature review," *Theor. Issues Ergonom. Sci.*, vol. 22, no. 2, pp. 1–14, 2020, doi: 10.1080/1463922X.2020.1801886.

[7] A. Gilchrist, *Industry 4.0: The Industrial Internet of Things*, 1st ed. New York, NY, USA: Apress, 2016.
[8] K. Darvish, E. Simetti, F. Mastrogiovanni, and G. Casalino, "A hierarchical architecture for human–robot cooperation processes," *IEEE Trans. Robot.*, vol. 37, no. 2, pp. 567–586, Apr. 2021.
[9] L. Gualtieri, E. Rauch, and R. Vidoni, "Emerging research fields in safety and ergonomics in industrial collaborative robotics: A systematic literature review," *Robot. Comput.-Integr. Manuf.*, vol. 67, Feb. 2021, Art. no. 101998. [Online]. Available: http://www.sciencedirect.com/science/article/pii/S073658452030209X
[10] C. Cimini, F. Pirola, R. Pinto, and S. Cavalieri, "A human-in-the-loop manufacturing control architecture for the next generation of production systems," *J. Manuf. Syst.*, vol. 54, pp. 258–271, Jan. 2020. [Online]. Available: http://www.sciencedirect.com/science/article/pii/S0278612520300029
[11] Y. Tirupachuri, "Enabling human-robot collaboration via holistic human perception and partner-aware control," Ph.D. dissertation, Bioeng. Robot., Curriculum Cogn. Robot., Interact., Rehabil. Technol., Univ. Genoa, Genoa, Italy, Apr. 2020. [Online]. Available: https://arxiv.org/abs/2004.10847
[12] Y. Hu, M. Benallegue, G. Venture, and E. Yoshida, "Interact with me: An exploratory study on interaction factors for active physical human-robot interaction," *IEEE Robot. Autom. Lett.*, vol. 5, no. 4, pp. 6764–6771, Oct. 2020.
[13] M. A. Gull, S. Bai, and T. Bak, "A review on design of upper limb exoskeletons," *Robotics*, vol. 9, no. 1, p. 16, Mar. 2020. [Online]. Available: https://www.mdpi.com/2218-6581/9/1/16
[14] R. Bostelman, Y.-S. Li-Baboud, A. Virts, S. Yoon, and M. Shah, "Towards standard exoskeleton test methods for load handling," in *Proc. Wearable Robot. Assoc. Conf. (WearRAcon)*, Mar. 2019, pp. 21–27.
[15] C. Latella, Y. Tirupachuri, L. Tagliapietra, L. Rapetti, B. Schirrmeister, J. Bornmann, D. Gorjan, J. Čamernik, P. Maurice, L. Fritzsche, J. Gonzalez-Vargas, S. Ivaldi, J. Babič, F. Nori, and D. Pucci, "Analysis of human whole-body articular stresses during overhead work with a passive exoskeleton," *IEEE Trans. Human-Mach. Syst.*, to be published.
[16] A. Colim, C. Faria, A. C. Braga, N. Sousa, L. Rocha, P. Carneiro, N. Costa, and P. Arezes, "Towards an ergonomic assessment framework for industrial assembly workstations—A case study," *Appl. Sci.*, vol. 10, no. 9, p. 3048, Apr. 2020.
[17] W. Kim, M. Lorenzini, P. Balatti, P. D. H. Nguyen, U. Pattacini, V. Tikhanoff, L. Peternel, C. Fantacci, L. Natale, G. Metta, and A. Ajoudani, "Adaptable workstations for human-robot collaboration: A reconfigurable framework for improving worker ergonomics and productivity," *IEEE Robot. Autom. Mag.*, vol. 26, no. 3, pp. 14–26, Sep. 2019.
[18] A. Ajoudani, P. Albrecht, M. Bianchi, A. Cherubini, S. Del Ferraro, P. Fraisse, L. Fritzsche, M. Garabini, A. Ranavolo, P. H. Rosen, M. Sartori, N. Tsagarakis, B. Vanderborght, and S. Wischniewski, "Smart collaborative systems for enabling flexible and ergonomic work practices [industry activities]," *IEEE Robot. Autom. Mag.*, vol. 27, no. 2, pp. 169–176, Jun. 2020.
[19] L. Roveda, S. Haghshenas, M. Caimmi, N. Pedrocchi, and L. Molinari Tosatti, "Assisting operators in heavy industrial tasks: On the design of an optimized cooperative impedance fuzzy-controller with embedded safety rules," *Frontiers Robot. AI*, vol. 6, p. 75, Aug. 2019. [Online]. Available: https://www.frontiersin.org/article/10.3389/frobt.2019.00075
[20] D. J. Agravante, A. Cherubini, A. Sherikov, P.-B. Wieber, and A. Kheddar, "Human-humanoid collaborative carrying," *IEEE Trans. Robot.*, vol. 35, no. 4, pp. 833–846, Aug. 2019.
[21] A. Mauri, J. Lettori, G. Fusi, D. Fausti, M. Mor, F. Braghin, G. Legnani, and L. Roveda, "Mechanical and control design of an industrial exoskeleton for advanced human empowering in heavy parts manipulation tasks," *Robotics*, vol. 8, no. 3, p. 65, Aug. 2019.
[22] D. Stanev, K. Filip, D. Bitzas, S. Zouras, G. Giarmatzis, D. Tsaopoulos, and K. Moustakas, "Real-time musculoskeletal kinematics and dynamics analysis using marker- and IMU-based solutions in rehabilitation," *Sensors*, vol. 21, no. 5, p. 1804, Mar. 2021.
[23] L. Fortini, M. Lorenzini, W. Kim, E. De Momi, and A. Ajoudani, "A real-time tool for human ergonomics assessment based on joint compressive forces," in *Proc. 29th IEEE Int. Conf. Robot Hum. Interact. Commun. (RO-MAN)*, Aug. 2020, pp. 1164–1170.
[24] C. Latella, S. Traversaro, D. Ferigo, Y. Tirupachuri, L. Rapetti, F. J. A. Chavez, F. Nori, and D. Pucci, "Simultaneous floating-base estimation of human kinematics and joint torques," *Sensors*, vol. 19, no. 12, p. 2794, Jun. 2019.
[25] C. Latella, "Human whole-body dynamics estimation for enhancing physical human-robot interaction," Ph.D. dissertation, Bioeng. Robot., Curriculum Cogn. Robot., Interact., Rehabil. Technol., Univ. Genoa, Genoa, Italy, Apr. 2018. [Online]. Available: https://arxiv.org/abs/1912.01136
[26] L. V. der Spaa, M. Gienger, T. Bates, and J. Kober, "Predicting and optimizing ergonomics in physical human-robot cooperation tasks," in *Proc. IEEE Int. Conf. Robot. Autom. (ICRA)*, May 2020, pp. 1799–1805.
[27] L. Rapetti, Y. Tirupachuri, A. Ranavolo, T. Kawakami, T. Yoshiike, and D. Pucci, "Shared control of robot-robot collaborative lifting with agent postural and force ergonomic optimization," in *Proc. IEEE Int. Conf. Robot. Autom. (ICRA)*, Apr. 2021. [Online]. Available: https://arxiv.org/abs/2104.13630
[28] S. Haddadin, A. De Luca, and A. Albu-Schäffer, "Robot collisions: A survey on detection, isolation, and identification," *IEEE Trans. Robot.*, vol. 33, no. 6, pp. 1292–1312, Dec. 2017.
[29] G. Cheng, E. Dean-Leon, F. Bergner, J. R. G. Olvera, Q. Leboutet, and P. Mittendorfer, "A comprehensive realization of robot skin: Sensors, sensing, control, and applications," *Proc. IEEE*, vol. 107, no. 10, pp. 2034–2051, Oct. 2019.
[30] X. Liu, G. Zuo, J. Zhang, and J. Wang, "Sensorless force estimation of end-effect upper limb rehabilitation robot system with friction compensation," *Int. J. Adv. Robotic Syst.*, vol. 16, no. 4, Jul. 2019, Art. no. 172988141985613, doi: 10.1177/1729881419856132.
[31] F. Nori, S. Traversaro, J. Eljaik, F. Romano, A. Del Prete, and D. Pucci, "ICub whole-body control through force regulation on rigid non-coplanar contacts," *Frontiers Robot. AI*, vol. 2, p. 6, Mar. 2015. [Online]. Available: https://www.frontiersin.org/article/10.3389/frobt.2015.00006
[32] A. Del Prete, L. Natale, F. Nori, and G. Metta, "Contact force estimations using tactile sensors and force/torque sensors," in *Proc. Conf., Hum.-Robot Interact. (HRI), Workshop Adv. Tactile Sens. Touch Based Hum.-Robot Interact.* Boston, MA, USA: ACM/IEEE, 2012, pp. 1–2. [Online]. Available: https://www.researchgate.net/publication/236152161_Contact_Force_Estimations_Using_Tactile_Sensors_and_Force_Torq ue_Sensors
[33] M. Lorenzini, W. Kim, E. De Momi, and A. Ajoudani, "An online method to detect and locate an external load on the human body with applications in ergonomics assessment," *Sensors*, vol. 20, no. 16, p. 4471, Aug. 2020.
[34] A. Spilz, T. Engleder, M. Munz, and M. Karge, "Development of a smart fabric force-sensing glove for physiotherapeutic applications," *Current Directions Biomed. Eng.*, vol. 5, no. 1, pp. 513–515, Sep. 2019, doi: 10.1515/cdbme-2019-0129.
[35] J. Hughes, A. Spielberg, M. Chounlakone, G. Chang, W. Matusik, and D. Rus, "A simple, inexpensive, wearable glove with hybrid resistive-pressure sensors for computational sensing, proprioception, and task identification," *Adv. Intell. Syst.*, vol. 2, no. 6, Jun. 2020, Art. no. 2000002.
[36] V. A. Spector and H. Flashner, "Modeling and design implications of noncollocated control in flexible systems," *J. Dyn. Syst., Meas., Control*, vol. 112, no. 2, pp. 186–193, Jun. 1990.
[37] R. Featherstone, *Rigid Body Dynamics Algorithms*. Secaucus, NJ, USA: Springer, 2007.
[38] C. Latella, M. Lorenzini, M. Lazzaroni, F. Romano, S. Traversaro, M. A. Akhras, D. Pucci, and F. Nori, "Towards real-time whole-body human dynamics estimation through probabilistic sensor fusion algorithms," *Auto. Robots*, vol. 43, no. 6, pp. 1591–1603, Aug. 2019, doi: 10.1007/s10514-018-9808-4.
[39] F. Nori, N. Kuppuswamy, and S. Traversaro, "Simultaneous state and dynamics estimation in articulated structures," in *Proc. IEEE/RSJ Int. Conf. Intell. Robots Syst. (IROS)*, Sep. 2015, pp. 3380–3386.
[40] L. Rapetti, Y. Tirupachuri, K. Darvish, S. Dafarra, G. Nava, C. Latella, and D. Pucci, "Model-based real-time motion tracking using dynamical inverse kinematics," *Algorithms*, vol. 13, no. 10, p. 266, Oct. 2020.
[41] B. Serrien, K. Aliaj, and T. Pataky, "A comparison of three-dimensional rotation formalisms for least-squares and Bayesian inverse kinematics," *OSF Preprints*, to be published. [Online]. Available: https://osf.io/z3ftr
[42] B. Serrien, T. Pataky, J.-P. Baeyens, and E. Cattrysse, "Bayesian vs. least-squares inverse kinematics: Simulation experiments with models of 3D rigid body motion and 2D models including soft-tissue artefacts," *J. Biomech.*, vol. 109, Aug. 2020, Art. no. 109902.
[43] D. E. Orin, A. Goswami, and S.-H. Lee, "Centroidal dynamics of a humanoid robot," *Auto. Robot.*, vol. 35, nos. 2–3, pp. 161–176, 2013.
[44] S. Traversaro and A. Saccon, "Multibody dynamics notation (version 2)," Dept. Mech. Eng. Technische Universiteit Eindhoven, Eindhoven, The Netherlands, Tech. Rep. DC2019.100, Nov. 2019. [Online]. Available: https://research.tue.nl/en/publications/multibody-dynamics-notation-version-2

[45] S. M. Bruijn, O. G. Meijer, J. H. van Dieën, I. Kingma, and C. J. C. Lamoth, "Coordination of leg swing, thorax rotations, and pelvis rotations during gait: The organisation of total body angular momentum," *Gait Posture*, vol. 27, no. 3, pp. 455–462, Apr. 2008.
[46] G. Metta, P. Fitzpatrick, and L. Natale, "YARP: Yet another robot platform," *Int. J. Adv. Robotic Syst.*, vol. 3, no. 1, p. 8, Mar. 2006.
[47] E. Svertoka, S. Saafi, A. Rusu-Casandra, R. Burget, I. Marghescu, J. Hosek, and A. Ometov, "Wearables for industrial work safety: A survey," *Sensors*, vol. 21, no. 11, p. 3844, Jun. 2021.
[48] T. Varrecchia, C. De Marchis, F. Draicchio, M. Schmid, S. Conforto, and A. Ranavolo, "Lifting activity assessment using kinematic features and neural networks," *Appl. Sci.*, vol. 10, no. 6, p. 1989, Mar. 2020.
[49] C. Di Natali, G. Chini, S. Toxiri, L. Monica, S. Anastasi, F. Draicchio, D. Caldwell, and J. Ortiz, "Equivalent weight: Connecting exoskeleton effectiveness with ergonomic risk during manual material handling," *Int. J. Environ. Res. Public Health*, vol. 18, no. 5, p. 2677, Mar. 2021.

YESHASVI TIRUPACHURI (Member, IEEE) received the B.Sc. degree in electrical and electronics engineering from Pondicherry Engineering College, Pondicherry, India in 2011, the M.Sc. degree in advanced robotics from the École Centrale de Nantes, Nantes, France, in 2014, and the M.Sc. degree in robotics engineering the Ph.D. degree in bioengineering and robotics from the University of Genoa, Genova, Italy, in 2015 and 2020, respectively. Since then, he has been a Postdoctoral Researcher with the Italian Institute of Technology (IIT), Genova. He was awarded the European Union's (EU) Marie Skłodowska-Curie Actions early stage researcher fellowship, and he contributed to EU H2020 funded PACE, and An.Dy projects. His research interests include human–robot interaction and collaboration, control theory, and wearable technology.

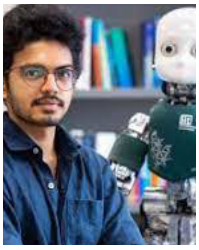

PRASHANTH RAMADOSS (Member, IEEE) received the B.Eng. degree in electronics and communication engineering from Anna University, Chennai, India, in 2013, the M.Sc. degree in advanced robotics from the École Centrale de Nantes, Nantes, France, in 2014, and the M.Sc. degree in robotics engineering from the University of Genoa, Genova, Italy, in 2015. Since 2018, he has been a Ph.D. Fellow at the University of Genoa and the Italian Institute of Technology (IIT), Genova. His research interests include control and state estimation for humanoid robots.

LORENZO RAPETTI (Member, IEEE) received the bachelor's and master's degrees *(cum laude)* in biomedical engineering from the Politecnico di Milano, Italy, in 2015 and 2017, respectively, and the master's degree in bioengineering from the University of Illinois at Chicago, USA, in 2017. He is currently pursuing the Ph.D. degree with The University of Manchester, Manchester, U.K. Since 2018, he has been a Researcher with the Dynamic Interaction Control Lab, Istituto Italiano di Tecnologia (IIT), working on humanoid robot control for human–robot interaction within the EU project An.Dy. and a joint lab with the Honda Research Institute Japan.

CLAUDIA LATELLA (Member, IEEE) received the B.Eng. degree in biomedical engineering from the University of Genoa, Genova, Italy, in 2009, the M.Eng. degree *(cum laude)* in bioengineering from the University of Genoa, in 2011, with an experimental mechanical thesis carried out at DynaMat Laboratories, University of Applied Sciences and Arts of Southern Switzerland (SUPSI), Lugano, dealing with the mechanical tensile behavior of bovine bones. After a working period, she came back to the academic environment and obtained the Ph.D. title in robotics from the University of Genoa, in 2018. Since then, she has been a Postdoctoral Researcher with the Dynamic Interaction Control (DIC) Lab, Istituto Italiano di Tecnologia (IIT). She is currently involved in the European project An.Dy. H2020-ICT (http://www.andy-project.eu). Her primary research interests include simultaneous multimodal sensor fusion algorithms for human kinematics and dynamics measurements.

KOUROSH DARVISH (Member, IEEE) received the B.Sc. degree in aerospace engineering from the K. N. Toosi University of Technology, Tehran, Iran, in 2012, the M.Sc. degree in aerospace engineering from the Sharif University of Technology, Tehran, in 2014, and the Ph.D. degree in bioengineering and robotics from the University of Genoa, Genova, Italy, in 2019. He is currently a Postdoctoral Researcher with the Italian Institute of Technology (IIT), Genova. So far, he has authored or coauthored several international journal and conference papers. During his postdoctoral research at IIT, he has contributed to the EU H2020 An.Dy. project and H2020 SoftManBot project on human–robot collaboration. His research interests include human–robot collaboration, telexistence, task representation, and robot motion planning and control.

SILVIO TRAVERSARO (Member, IEEE) received the B.Eng. and M.Eng. degrees (Hons.) in computer science and robotics engineering and the Ph.D. degree in robotics from the University of Genoa, Genova, Italy, in 2011, 2013, and 2017, respectively. He is currently with the Italian Institute of Technology (IIT), Genova, involved in dynamics modeling, estimation, and identification applied to the iCub robot, where he has been a Postdoctoral Researcher, involved in industrial and commercial applications of robotics.

DANIELE PUCCI (Member, IEEE) received the bachelor's and master's degrees (Hons.) in control engineering from the Sapienza University of Rome, Rome, Italy, in 2007 and 2009, respectively, and the Ph.D. degree in nonlinear control applied to flight dynamics, with a thesis prepared with INRIA Sophia Antipolis, Valbonne, France, in 2013, under the supervision of Tarek Hamel and Claude Samson. From 2013 to 2017, he has been a Postdoctoral Researcher with the Istituto Italiano di Tecnologia (IIT), working within the EU project CoDyCo. Since August 2017, he has been the Head of the Dynamic Interaction Control Lab. Also, the lab is pioneering aerial humanoid robotics, whose main aim is to make flying humanoid robots. The lab is currently implementing iRonCub, the jet-powered flying version of the humanoid robot iCub. He is also the Scientific PI of the H2020 European Project Andy, the Task Leader of the H2020 European Project SoftManBot, and a Coordinator of the joint laboratory between IIT and Honda JP. Since 2020 and in the context of the split-site Ph.D. supervision program, he has been a Visiting Lecturer with The University of Manchester, Manchester, U.K. His research interests include humanoid robot locomotion problem with specific attention on the control and planning of the associated nonlinear systems. He was a recipient of the Academic Excellence Award from Sapienza, in 2009, and also awarded as the Innovator of the Year Under 35 Europe from the *MIT Technology Review* Magazine, in 2019.